Biological and Medical Applications of Materials and Interfaces

MOF-based enzymatic microfluidic biosensor via surface patterning and biomineralization

Munirah Izzah Binti Mohammad, Amir Razmjou, Kang Liang, Mohsen Asadnia, and Vicki Chen

ACS Appl. Mater. Interfaces, **Just Accepted Manuscript** • DOI: 10.1021/acsami.8b16837 • Publication Date (Web): 07 Dec 2018

MOF-based Enzymatic Microfluidic Biosensor *via* Surface Patterning and Biomineralization

Munirah Mohammad[†], Amir Razmjou[¥†], Kang Liang[†#], Mohsen Asadnia[‡] and Vicki Chen[†+*]*

[†]UNESCO Centre for Membrane Science and Technology, School of Chemical Engineering, University of New South Wales, Sydney 2052, Australia

[¥]Department of Biotechnology, Faculty of Advanced Sciences and Technologies, University of Isfahan, Isfahan 73441-81746, Iran

[#]Graduate School of Biomedical Engineering, University of New South Wales, Sydney 2052, Australia

[‡]School of Engineering, Macquarie University, Sydney, 2109, Australia

[+]School of Chemical Engineering, University of Queensland, St. Lucia, 4072, Australia

ABSTRACT: Recently, the biomineralization of enzyme in metal-organic-framework (enzyme-MOF) composite have shown a great potential to increase enzymes stability without compromising their activity; hence, it is desirable for its applications in bio-sensing devices. Nonetheless, most of the enzyme-MOF research has been focusing on enzyme encapsulation in particle form, which limits its synthesis flexibility for practical applications; due to its requirement for post-synthesis immobilization onto solid support. Therefore, to develop a diagnostic device out of the biomineralized enzyme, surface patterning and integration of microfluidic system offers many advantages. In this work, mussel-inspired polydopamine/polyethyleneimine (PDA/PEI) coating is employed to pattern enzyme-MOF in microfluidic channels and exploit the wettability gradient for "pumpless transportation" effect. As a proof of concept, we combine a cascade reaction of glucose oxidase (GOx) and horseradish peroxidase (HRP) enzymes to detect glucose into a patterned zeolitic imidazole

framework - 8 (ZIF-8) thin film on a flexible polymeric substrate. The results show that the ZIF-8/GOx&HRP *in-situ* composites on PDA/PEI patterns have good acid and thermal stability compared to samples without ZIF-8. ZIF-8/GOx&HRP *in-situ* shows high selectivity towards glucose, linear sensitivity of 0.00303 Abs/μM and the Limit of Detection (LoD) of 8 μM glucose concentration. An unexpected benefit of this approach is the ability of the ZIF-8 thin film structure to provide a diffusion limiting effect for substrate influx; thus, producing high range of linear response range (8 μM-5mM of glucose). This work provides insight on the spatial location of the enzymes in MOF thin films; and the potential of such patterning techniques for MOF-based biosensors using other types of biological elements such as antibodies and aptamers.

KEYWORDS: microfluidic, biosensors, metal-organic framework, patterning, enzymes, polydopamine, pumpless transportation

1. Introduction

Over the years, enzyme-based biosensors have been an attractive analytical tool to a wide variety of applications such as in biomedical fields (medical diagnostic and monitoring) and food safety (allergen detections). Using enzymes as the primary biological sensing element poses the benefits of high sensitivity and high selectivity towards their target analytes.[1] However, the use of enzyme suffers from major drawbacks of poor chemical, thermal, mechanical and long-term storage stability.[1] These limitations can be attributed to the susceptibility of enzymes to immobilization and operating conditions such as high temperature, low pH and exposure to non-biocompatible organic solvent.[2] Due to these instabilities, extensive applications of enzymes in devices are constrained.

Recently, the *in-situ* biomineralization of enzymes using metal-organic-framework (MOF) has shown a great potential in increasing enzymes stability without compromising their activity and performance.[2-4] *In-situ* enzyme-MOF synthesis is understood as the nucleation and growth of MOF which happens concurrently with the enzyme immobilization in a one-step approach, resulting in crystallization of MOF with embedded enzyme either at the particle surface, or within the framework.[5] One of the notable works in this field has been done by Liang et al.,[2] which demonstrates a water based approach for immobilizing enzymes in MOF, particularly the zeolitic imidazole framework - 8 (ZIF-8).[2] It was demonstrated that the enzyme-MOF particle composite maintains the activity of the enzyme in high temperature (100^{o}C), and in the presence of enzyme inhibitors.[2]

Nonetheless, most of the enzyme-MOF research revolves around synthesizing enzyme-MOF composites in free particle systems in which, the enzyme-MOF composites were mixed with analytes and then, filtered out from the solution prior to analysis.[5-8] The issue with handling enzyme-MOF in particle form is that it requires an additional step of immobilizing the post-synthesized enzyme-MOF composite onto a solid substrate for

application such as in biosensing. This process is tedious and will restrict the particles immobilization mechanism to weak physical adsorption. Previously, an attempt has been made to facilitate *in-situ* MOF growth on a solid surface *via* protein-induced biomineralization. Liang et al. has first reported the nucleation of ZIF-8 on protein rich patterns on various substrates.[9] The presence of protein has been shown to accelerate the agglomeration of metal-cations and ligand; thus, acting as a nucleating agent for ZIF-8.[9] Since then, various enzyme-MOF patterning approaches including using commercial inkjet printing have emerged.[10] During enzyme-MOF based device fabrication, it is crucial to pre-treat the surface with a binding agent in order to achieve better stability and integrity of the enzyme-MOF layer.

To realize the potential of MOF-based enzymatic biosensors, a simple and rapid fabrication of robust enzyme-MOF thin film on solid surfaces are required. Therefore, in this paper, a mussel inspired polydopamine/polyethyleneimine (PDA/PEI) patterning is employed to induce nucleation of enzyme-MOF composite on polypropylene (PP) substrate. Polydopamine which was found to adhere to hydrophobic surfaces *via* electrostatic and hydrophobic interactions, contains an abundance of catechol containing compound such as 3,4-dihydroxyphenyl-L-alainine (DOPA) and lysine.[11-12] During paired polymerization of PDA/PEI, PEI undergoes Michael addition or Schiff-base reactions with catechol group in PDA to form a robust bio-adhesive layer on the polymeric substrate.[13-14] In this context, PEI was used as a cross linking agent with PDA,[15] and it was shown to increase the mechanical integrity of the PDA/PEI film,[16-17] while reducing the coating time and increases its hydrophilicity.[18] The increase in hydrophilicity of PDA/PEI surface is due to the contribution of positive charges by PEI which is also an amino-rich polycation.[12]

It is important to highlight that, the PDA/PEI surfaces can induce biomineralization process on the solid liquid inteface.[13, 19] The mechanism of ZIF-8 biomineralization is first by

the precursors enrichment on the hydrophilic PDA/PEI coating, followed by the chelation of zinc ion precursors on the surface via PDA's catechol moiety.[12] This enable the heterogenous nucleation and growth of ZIF-8 on the surface of PDA/PEI coating.[20-22] Without the presence of PDA/PEI intermediate layer, homogenous nucleation is preferred in bulk solution hindering the ability to form ZIF-8 thin film layer on the surface of the inert hydrophobic polymeric substrate. Therefore, it is expected that the enzyme-MOF composites will biomineralize *in-situ* in the form of thin films on the PDA/PEI coating.

Although PEI is toxic by itself, the toxicity level is not detrimental to the enzymes when modified with PDA. Recent paper by Zhang et al.[23] has shown that not only enzyme is compatible to be used with PEI grafted on PDA coating, the activity of enzyme glucose oxidase (GOx) is the highest when immobilized with PEI on PDA coating, compared to other enzyme immobilization reagent using glutaraldehyde and 1-dodecanethiol.[23] It is worth to note that the overall PDA/PEI coating offers anti-bacterial effect and demonstrate compatibility with biomolecule including enzyme;[14, 24-25] thus, justifying the use of bio-inspired material for this design.

As alluded earlier, PDA/PEI coating can alter the wettability of a hydrophobic surface to hydrophilic properties. Conventional microfluidic paper-based biosensors have always utilized dual surface wettability; a hydrophilic part for enzyme attachment and liquid retention; and a hydrophobic barrier for liquid confinement in the hydrophilic part.[26] The fabrication process of such device focuses on patterning a hydrophobic coating such as paraffin wax[27] or trimethoxy octadecylsilane (TMOS)[28] onto an inherently hydrophilic filter paper. Nonetheless, due to the high melting point of the materials, the integration of the hydrophobic pattern onto the filter paper requires heat press treatment, adding an additional processing step. In contrast, we use a hydrophobic polypropylene (PP) membrane as a substrate material and apply a hydrophilic PDA/PEI patterning using a reusable

polydimethylsiloxane (PDMS) microfluidic channels at room temperature. The difference between surface wettability of the hydrophilic PDA/PEI patterning and hydrophobic PP membrane creates a surface free energy gradient, which drives the liquid movement on the PDA/PEI patterns *via* capillary forces. This eliminates the need to use external equipment for pumping mechanism which simplifies the setup and reduces the cost of the device. The "pumpless transportation" mechanism utilizing hydrophilic patterning on hydrophobic substrates was demonstrated in our previous work.[29]

The PP polymer is intrinsically hydrophobic due to the presence of -CH- and -CH_2- backbone, and -CH_3 pendant group and can used directly as hydrophobic support from manufacturers to enable "pumpless transportation'. It is also suitable to be used as a paper-based biosensor as it is an inexpensive, low density flexible material. Besides that, the porous morphology of PP membrane surfaces is ideal for the adhesion of PDA/PEI layer. Therefore, it is not preferred to use other solid hydrophobic supports without such morphology. Lastly, it was reported that PP has shown better biocompatibility compared to other hydrophobic polymers used in biomedical applications such as polytetrafluoroethylene and polyester.[30] Due to its desirable structural properties and biocompatibility, PP membrane is justified to be used as a base support in this study.

In addition to enabling the fabrication of portable lab-on-chip (LOC) concept devices, the integration of microfluidic systems in biosensor devices offers significant advantages such as reduction in the number of samples, amount of chromogen reagent and energy consumption.[1, 31] For commercialization purposes, a facile patterning technique using microfluidic system will benefit the flow of production and consistency of the product. It will also assist the incorporation of MOF into enzyme-based biosensor through biomineralization process.

As a model enzyme and proof of concept, we used a combination of glucose oxidase (GOx) and horseradish peroxidase (HRP) to detect glucose. According to International Diabetes Federation (IDF), it is estimated that 8.4 % of the global population aged 18-99 years suffers from diabetes in 2017, and this number is expected to increase to 9.9 % in 2045.[32] The rising number of diabetes patients with the need to monitor the blood glucose level daily results in a plethora of glucose sensing point-of-care (PoC) devices in market.[33] Therefore, the enzyme-MOF glucose biosensor can be as a proof of experiment; before paving the way for synthesis of other type of biosensors in this field.

In this paper, the enzymatic cascade of reaction or multi-enzyme systems is essential for colorimetry detection, which relies on monitoring the formation of colored products that can be recognized by naked eyes or optical sensing instrument such as spectrophotometer. The colored intensity measured by the absorbance wavelength is proportional to the concentration of products in the solution. The GOx and HRP are used in tandem for glucose detection via cascades of reaction which are: 1) the conversion of glucose ($C_6H_{12}O_6$) to gluconic acid catalyzed by GOx with the presence of oxygen, producing hydrogen peroxidase (H_2O_2) as by-product; and 2) the H_2O_2 is converted to water by catalyzed reaction of HRP. With the presence of chromogen 2,2'-azino-bis(3-ethylbenzothiazoline-6-sulphonic acid) (ABTS), reaction (2) will subsequently oxidize $ABTS^{-2}$ to $ABTS^{\bullet-}$ which can be detected at 415 nm by spectrophotometer or appears as visible green color by naked eye. Without the presence of second enzyme HRP and chromogen ABTS, there are no other means of detection via colorimetry for the products of reaction (1) only. Therefore, the cascade reactions of GOx and HRP are crucial for detection based on color change.

In a broader context, we have demonstrated the feasibility of enzymatic cascade reactions in enzyme-MOF thin films that can be extended in other applications. The multi-enzyme systems has received attention of researchers for myriad applications,[7, 34] such as in

enzymatic fuel cell,[35] carbon capture and conversion,[14, 36] drug synthesis,[37] and biosensing.[7] In general, the enzymatic cascade reaction is limited by the proximity of enzymes between each other for substrate transfer. Therefore, tandem immobilization of enzyme can increase the overall enzymatic activity due to improved mass transfer of substrates to the active site of the enzyme.[38] By utilizing ZIF-8/GOx&HRP in-situ biomineralization; enzymes are in the close proximity of each other, hence, demonstrating the feasibility of cascade reaction with this synthesis technique. This method can be extended to other type of enzymatic cascade-based sensors for lactase and amylase detection in a form of 3 – in – 1 LoC devices.

Herein, the mussel-inspired PDA/PEI patterning is employed to induce biomineralization of enzyme-MOF composite on PP substrate; particularly ZIF-8/GOx&HRP thin film. The role of the microfluidic system is to provide a containment for patterning and ZIF-8/GOx&HRP precursor solution. Combining two known technologies of *in-situ* biomineralization and microfluidic systems into one, we study the characteristic of the ZIF-8/GOx&HRP patterning and its performance to be used as a reliable glucose biosensor. Various characterization techniques such as scanning electron microscopy (SEM), Fourier-transform infrared-spectroscopy (FT-IR), thermogravimetric analysis (TGA), x-ray diffraction (XRD), inductively coupled plasma mass spectrometry (ICP-MS) and contact angle measurements have been used to demonstrate the effect of synthesis protocol to the structure. To study the role of ZIF-8 in the bio-composite patterning, the activity of the bio-composite with the exposure to acidic, high temperatures, and with presence of enzymatic inhibitors are analyzed. Finally, the performance of the bio-composites is evaluated in terms of selectivity, sensitivity, detection limits and the ability to produce a readout scheme for optical detection.

2. Results and Discussions

2.1. Fabrication of Bio-composite Patterning

The fabrication of bio-composite patterning of ZIF-8 and GOx&HRP is illustrated in **Figure 1**. A flexible PDMS mold with microfluidic channels is placed on top of the bare polypropylene (PP) membrane. Mussel inspired (polydopamine/polyethyleneimine) PDA/PEI patterning is achieved by injecting the mixture of ethanol, dopamine and PEI solution (Tris buffer, pH 8.5, 0.05 M) into the microchannels. The concentration of dopamine and PEI are both 2 mg/mL. The mixture is deposited on the PP membrane for 4 hours and rinsed thoroughly with Milli-Q® water. Afterwards, ZIF-8 precursors solutions (zinc nitrate hexahydrate, $Zn(NO_3)_2$, 0.0135 g and 2-methylimidazole, HMIM, 0.2830 g) with 0.4 mL of enzyme solutions (2 mg of glucose oxidase, GOx and 3 mg of horseradish peroxidase, HRP) are injected into the microchannels and left to react for 30 minutes. The simultaneous nucleation of ZIF-8 and immobilization of GOx&HRP in this method results in ZIF-8/GOx&HRP *in-situ* on the PDA/PEI patterning. As a control in studying the effect of presence of enzyme to the ZIF-8 thin film structure, ZIF-8 thin film on PDA/PEI patterning was synthesized using ZIF-8 precursor solutions for 30 minutes without the enzyme solution. The fabrication technique is illustrated in **Figure 1** and the details are included in the Experimental Section.

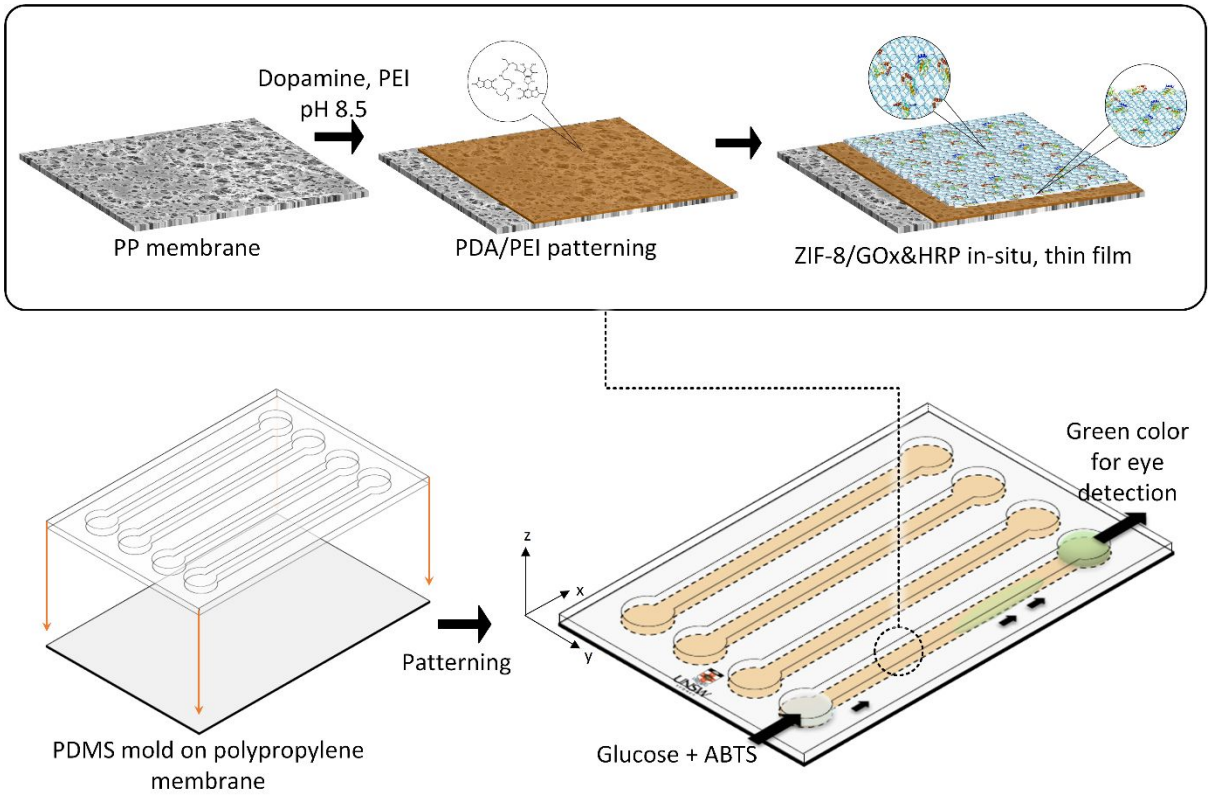

Figure 1. Schematic drawing of fabrication of bio-composite patterning. Bare polypropylene (PP) membrane is coated with polydopamine/polyethyleneimine (PDA/PEI) patterning using PDMS mold with microchannels. Then, ZIF-8/GOx&HRP *in-situ* in which the ZIF-8 and the enzyme GOx and HRP are co-precipitated on the PDA/PEI layer (*in-situ* growth).

With the goal of immobilizing enzyme-MOF matrix onto solid support *via* bio-adhesion through mussel-inspired PDA/PEI patterning, additional approaches were explored to demonstrate the flexibility in integrating the enzyme-MOF architecture in a device. Two alternative schemes which were explored are 1) the layer-by-layer method (LbL), in which the enzyme is first immobilized onto the PDA/PEI patterning before the synthesis of ZIF-8 over the PDA/PEI-enzyme surfaces; and 2) the deposition of pre-synthesized enzyme-MOF particles on the PDA/PEI patterning.

In theory, the layer by layer method will ensure complete protection of the enzyme underneath the MOF thin film; however, this is at the expense of additional mass transfer resistance between the analyte and the enzyme. In contrast with the proposed *in-situ* method, LbL method will require an additional step for fabrication.

Similar to the LbL method, the deposition of pre-synthesized enzyme-MOF particles on PDA/PEI patterning prolongs the fabrication process with the need to pre-synthesize the enzyme-MOF particles. Another disadvantage of using particle deposition method is the susceptibility of the particles to detachment as the immobilization mechanism is due to weak van der Waals forces between the hydrophobic ZIF-8 and the hydrophilic PDA/PEI surface. In a sense of comparing the alternative enzyme-MOF immobilizations on PDA/PEI (layer-by-layer and particle deposition), the performance each alternative scheme to provide color change within 10 minutes were observed. It was found that *in-situ* method has better performance for color change than the other schemes (results in **Figure S1**, Supporting information).

2.2. Surface characterization

Scanning electron microscopy (SEM) was employed to study the surface morphology of the modified PP membrane. **Figure 2a** shows the pores of pristine PP membranes are not visible due to the PDA/PEI patterning, indicating that the hydrophobic PP membrane is successfully covered by the hydrophilic layer of the PDA/PEI. Previously our group showed that the formation of PDA/PEI film on a porous polymeric membrane is stable and robust.[39] The cross-section images shows that the PDA/PEI is constructed as a thick, dense film on top of the PP membrane with an estimated thickness of 252 ± 99 nm (**Figure 2a**, insert and **Figure S2**, Supporting Information). Based on **Figure 2b** (ZIF-8 without enzyme)**,** the ZIF-8 crystals on PDA/PEI patterns forms a highly intergrown layer. Studying samples with reaction times show that the ZIF-8 crystals can be formed within 5 minutes; and the crystals are more intergrown as the synthesis time increases to 30 minutes (**Figure S3**, Supporting information). The presence of enzyme in the ZIF-8 precursor mix for ZIF-8/GOx&HRP *in-situ* approach results in a higher particle aggregation and a rougher surface morphology compared to the ZIF-8 crystals grown without enzyme (**Figure 2c**). Similarly, the ZIF-

8/GOx&HRP in-situ thin film layer shows time-dependent nucleation and growth on the PDA/PEI coating, with the first seeding can be observed clearly at 10 minutes and gradual growth of the intergrown ZIF-8/GOx&HRP in-situ film by 30 minutes (**Figure S4**, Supporting Information). It is also worth to mention that the presence of PDA/PEI patterning ensures more cohesive formation of ZIF-8/GOx&HRP *in-situ* as a thin film as shown in **Figure S5** (Supporting Information) compared to samples of ZIF-8/GOx&HRP *in-situ* without PDA/PEI intermediate layer.

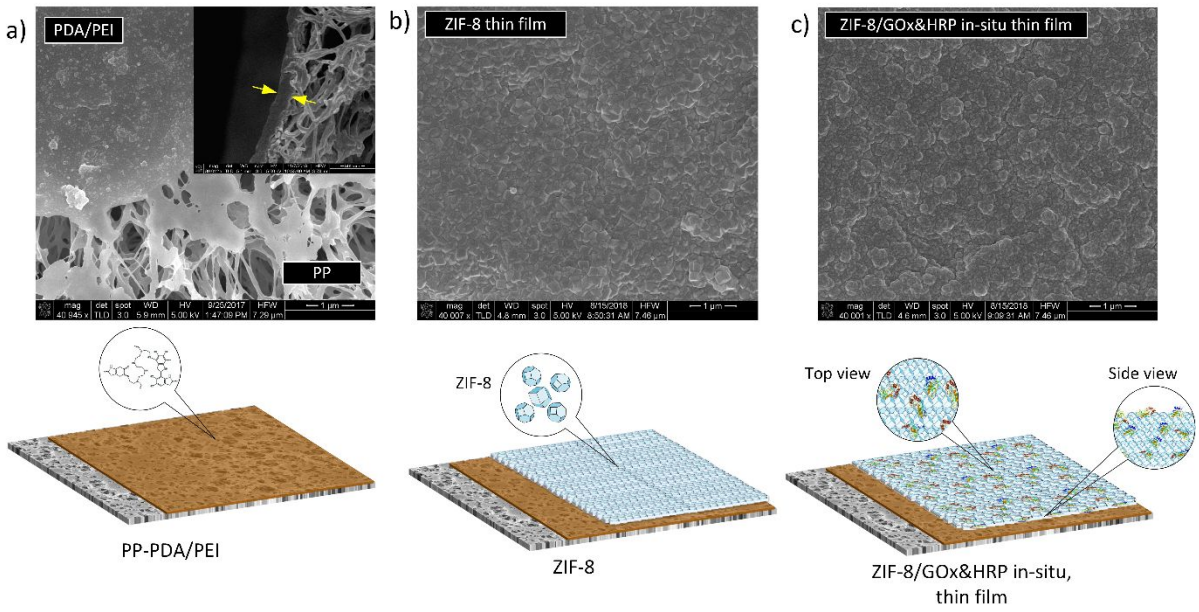

Figure 2. SEM image of a) PDA/PEI coatings on PP membrane with cross section insert showing PDA/PEI film; (b) formation of ZIF-8 without enzyme and c) formation of ZIF-8/GOx&HRP *in-situ*.

To estimate the thickness of ZIF-8/GOx&HRP *in-situ* patterning, the PP substrate was replaced with a silicon wafer to provide a solid support for atomic force microscopy (AFM) study. The silicon wafer was coated with PDA/PEI for 4 hours, followed by using the PDMS mold to create the ZIF-8/GOx&HRP *in-situ* patterning. Step analysis showed an average thickness of 62.5 nm for ZIF-8/GOx&HRP in-situ layer (**Figure 3a-c**). Next, the relative surface roughness was assessed for PDA/PEI, ZIF-8 and ZIF-8/GOx&HRP composites which resulted to be 5.19 ± 0.73 nm, 15.24 ± 1.92 nm and 9.90 ± 0.46 nm respectively (**Figure S6**,

Supporting information). The ZIF-8 and ZIF-8/GOx&HRP composites significantly change the surface roughness of the PDA/PEI patterning. The presence of enzyme in ZIF-8/GOx&HRP *in-situ* composites creates more fine and denser particles on the PDA/PEI patterns.

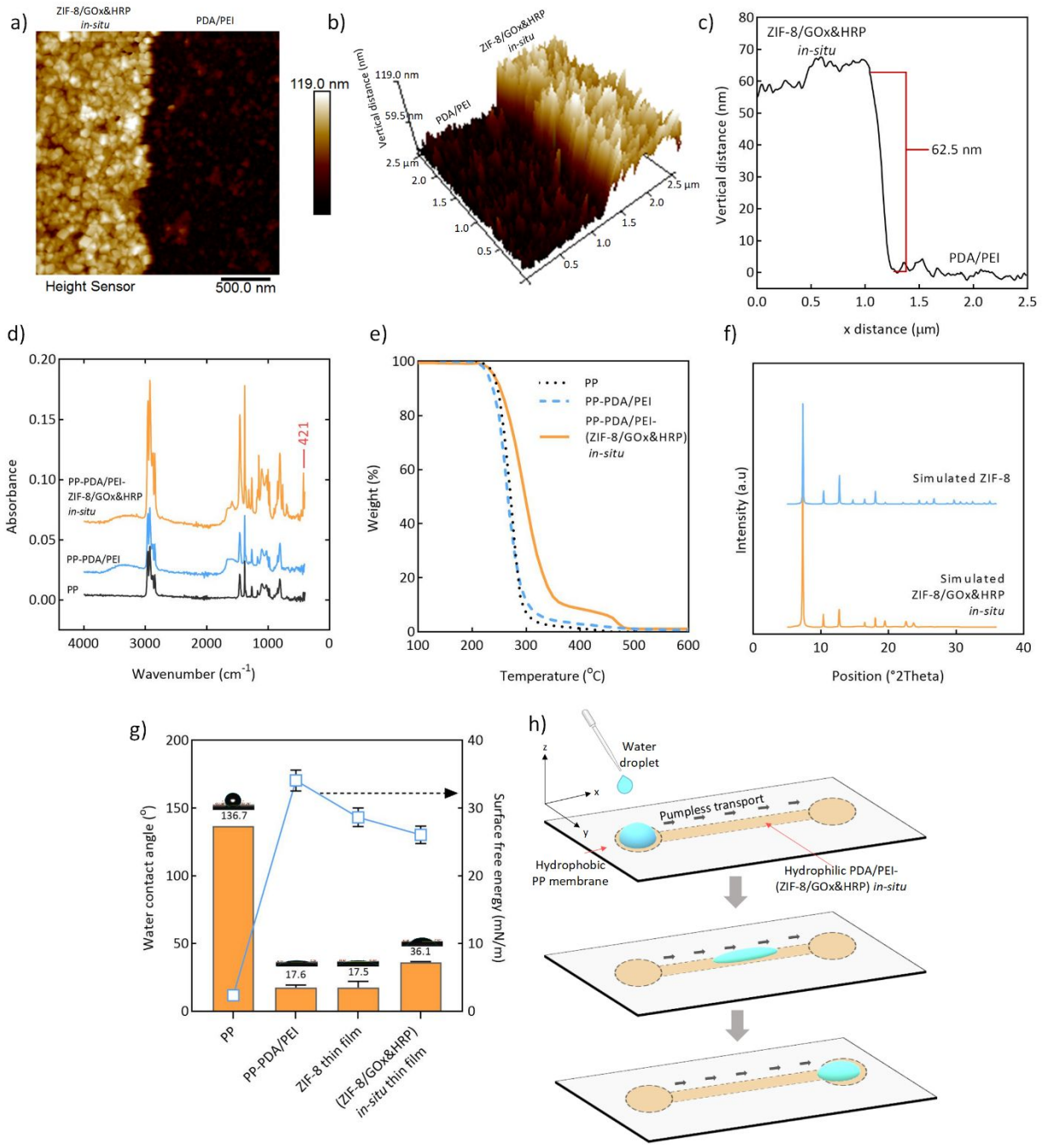

Figure 3. a-c) AFM results for ZIF-8/GOx&HRP *in-situ* patterning on PDA/PEI; a) 2-D Height Sensor image; b) 3-D Height Sensor image; and c) Step analysis. d) FT-IR results on ZIF-8/GOx&HRP *in-situ* showing characteristic ZIF-8 wavenumber at 421 cm^{-1}; e) TGA curve of ZIF-8/GOx&HRP *in-situ*; and f) XRD spectra of simulated peaks from ZIF-

8/GOx&HRP *in-situ* with simulated ZIF-8 from Powder Diffraction File 4 (PDF-4) organic database (reference ID: 00-062-1030);[40] g) Water contact angle results of the PP membrane compared with modifications (PDA/PEI, ZIF-8 thin film and ZIF-8/GOx&HRP *in-situ* thin film) with respective image data and calculated surface free energy of corresponding surfaces, with diiodomethane and glycerol, using Van Oss approach; h) schematics of liquid pumpless transportation application using hydrophilic patterning on hydrophobic base.

The Fourier Transform – IR (FT-IR) tests were performed to study the surface chemistry of the modified structure of PP membrane. The surface modified with PDA/PEI patterning resulted in a distinct and broad shape with IR band of 3200 – 3650 cm^{-1} which corresponds to stretches of alcohol, catechol and N-H bonds from the PDA and PEI structures (**Figure 3d** and **Figure S7a**, Supporting information). Biomineralization of ZIF-8 on the PDA/PEI patterning reveals 11 new peaks with the two notable peaks at 3133 cm^{-1} and 421 cm^{-1} which correspond to 1,2,5-oxadiazole and Zn-N stretching respectively (**Figure S7b**, Supporting information); with the latter being a characteristic peak of ZIF-8 as cited in the literature.[41] The presence of enzyme GOx and HRP in the ZIF-8/GOx&HRP *in-situ* patterning produced a small FT-IR peaks (**Figure S7c**, Supporting information) at 1636 and 1535 cm^{-1-} which is in proximate region of amide I vibration (1700-1600 cm^{-1}) and amide II vibration (1600-1500 cm^{-1}) respectively.[42-43] These are the characteristic vibrations of amino acid side chains of the enzyme secondary structure, which suggests that the enzymes are not denatured after biomineralization with ZIF-8.[42-43] The characteristic ZIF-8 peak at wavenumber of 421 cm^{-1} is also observed with ZIF-8/GOx&HRP *in-situ* (**Figure 3d**) which confirms the formation of ZIF-8 structure.

Next, we employed thermal gravimetric analysis (TGA) to study the decomposition rate of the bio-composite patterning and the results are shown in **Figure 3e** and **Figure S8a** (Supporting information). Decomposition of PDA/PEI patterned PP membrane (**Figure S8b**, Supporting information) exhibited similar curve to the pristine PP; however, with higher weight loss in the range 200-280 ^{o}C and higher residue after 450 ^{o}C, which indicates the

presence of PDA/PEI polymer. Similar trend was observed in the literature when PDA is coated onto PVDF membrane; in which, the PDA coated membrane exhibit higher weight loss in the beginning and higher residues at the end of the test.[44]

The TGA curve for synthetized ZIF-8 particles showed two steps of mass loss (**Figure S8d**, Supporting information); with the first step below 200 ^{o}C due to the release of the unreacted organic linker (2-methylimidazole) and guest molecules (mainly H_2O);[45-46] and the second step is at around 450 ^{o}C. This result is in agreement with previously published studies, for both steps of ZIF-8 thermal degradation.[45-46] A plateau over 500 ^{o}C can be attributed to the presence of zinc residue in the form of zinc oxide (ZnO). Then, the decomposition rate comparison of the ZIF-8 particles with the bio-composites pattern of ZIF-8 thin film (without enzyme) and ZIF-8/GOx&HRP *in-situ* thin film (with enzyme) were done (**Figure S8c**, Supporting information). There is an obvious second stage of weight loss at ~470 ^{o}C for ZIF-8/GOx&HRP *in-situ* (**Figure 3e** and **Figure S8c**, Supporting information)*;* which indicates that the decomposition of ZIF-8/GOx&HRP thin film occurs at a higher temperature than ZIF-8 particles. However, the second stage of mass loss is not observed for the TGA curve of ZIF-8 thin film without enzyme, implying lower ZIF-8 density on the sample. The percentage of ZIF-8 based on zinc residues in the ZIF-8/GOx&HRP *in-situ* composite is calculated to be 65.8 % higher than the residue from the ZIF-8 thin film without the presence of enzyme. This can be explained by an existing study which shows that the presence of proteins will speed up the precipitation of ZIF-8 crystals, leading to higher density of ZIF-8 to biomineralized on the PDA/PEI patterning.[2]

The X-ray diffraction (XRD) tests were conducted to identify the ZIF-8 structure on the bio composite patterns. For this purpose, the ZIF-8 and ZIF-8/GOx&HRP composites were synthetized for 5 hours to create sufficiently thick bio composite layer for the XRD tests. In **Figure S9a** (Supporting Information), the XRD patterns of PP-PDA/PEI-ZIF-8

consists of the broad peak by amorphous PP and PDA/PEI patterns and high intensity peaks which reflects the crystalline structure on the bio-composite. The XRD pattern confirms most of the major peaks exhibited by simulated ZIF-8 patterns.[40] Similarly, for ZIF-8/GOx&HRP *in-situ* composite, the distinct peaks identified are at position 2 theta of 7.3^{o}, 10.3^{o}, 12.7^{o} and 18.02^{o} with corresponding to 110, 200, 211 and 222 orientations respectively (**Figure 3f** and **Figure S9b,** Supporting Information). These are in good agreement with the simulated ZIF-8 patterns, which identify the presence of ZIF-8 crystal structure.

The enzyme loading can be estimated with inductively coupled plasma mass spectrometry (ICP-MS) from the amount of iron, Fe in the sample.[10] Since one molecule of enzyme HRP (mw~ 40000 Da) consists of one iron center, the enzyme loading (kg enzyme/kg PDA/PEI) percentage was calculated to be 20.9 % and 13.9 % for HRP and GOx respectively in PDA/PEI-GOx&HRP patterns (without ZIF-8). The ZIF-8/GOX&HRP *in-situ* had higher HRP and GOx loading of 34.0 % and 22.7 % respectively. These results support the hypothesis that higher enzymatic loading can be achieved with the biomineralization of enzyme on the PDA/PEI patterns.

As alluded earlier, dual-wettability properties of the hydrophilic patterned surface on the hydrophobic membrane is essential for liquid pumpless transportation. The wetting properties of the surface can be manipulated by altering the surface chemistry and surface microstructure. In **Figure 3g**, the water contact angle (WCA) and corresponding surface free energy (SFE) of modified surfaces are presented. The SFE can be calculated using acid-base approach by Van-Oss from contact angle measurement of water, glycerol and diiodomethane.[47] Schematics of the pumpless transportation application is shown in **Figure 3h** to highlight the importance of the wetting contrast.

Based on **Figure 3g**, the PDA/PEI patterning significantly lowers the WCA of PP from 136.7 ± 2.0 ^{o} to 17.6 ± 1.7 ^{o} while the SFE increases from 2.3 ± 0.16 mN m^{-1} to 34.1 ±

1.55 mN m^{-1}. These can be attributed to the change in the surface chemistry with an abundance of catechol group; hence, increasing the chemical affinity of the surface towards water molecules, making it more hydrophilic. The formation of ZIF-8 thin film and ZIF-8/GOx&HRP *in-situ* thin film slightly increases the WCA of the surface to 14.5 ± 4.5 ^{o} and 36.1 ± 0.6 ^{o}, respectively. The change in WCA in this case, is attributed to the formation of ZIF-8 microstructures which increases the surface roughness of the patterning, making it more hydrophobic. Interestingly, the reason for slightly lower WCA value for ZIF-8 thin film compared to than ZIF-8/GOx&HRP *in-situ* thin film, can be explained using the Wenzel model. This model states that, the roughness factor plays a role in amplifying the intrinsic surface wettability.[48-49] Previous observations of the SEM and AFM image of ZIF-8/GOx&HRP *in-situ* reveals fine and dense particles with lower surface roughness compared to ZIF-8 thin film (refer AFM results and Supporting information **Figure S6**). According to the Wenzel model, the lower roughness of hydrophilic surface leads to lower surface area for chemical affinity;[48-49] hence, the ZIF-8/GOx&HRP *in-situ* with lower surface roughness exhibit more hydrophobicity. This interesting observation suggests alternative wettability manipulation by changing the ZIF-8 microstructure using the presence of enzymes.

Nonetheless, it is apparent that the hydrophilic properties of PDA/PEI are dominant in both ZIF-8 and ZIF-8/GOx&HRP *in-situ* thin film samples. Exploiting hydrophilic patterning on hydrophobic surfaces (in this case, PDA/PEI patterning on PP membrane); have an attractive application as pumpless transport in the paper-based diagnostic device as discussed earlier (**Figure 3h** and **Supporting Information-Video**). The room temperature PDA/PEI patterning on the PP membrane offers a facile alternative approach compared to the conventional wax on paper fabrication devices for the same purpose as liquid containment.

2.3. Chemical, Thermal and Inhibitory Stability of ZIF-8/GOx&HRP in-situ Thin Film

Based on the literature,[2, 7-9, 50] we hypothesized that the biomineralized ZIF-8 will provide an entrapment for the enzyme on the PDA/PEI patterning; hence, increasing the chemical, thermal and inhibitor stability of the biomineralized enzyme. Therefore, the ZIF-8/GOx&HRP *in-situ* stability was tested in acid, at elevated temperature of 100 ^{o}C and with exposure to various inhibitors.

The pH value of physiological fluids such as blood, interstitial fluid, urine, sweat, saliva and ocular fluid ranges from pH 4.5 – 8.[33] In this study, a constant pH value of 5 was chosen to test the stability of the ZIF-8/GOx&HRP *in-situ* biosensor in exposure to the acidic conditions of physiological fluids. Next, evaluation of thermal stability is crucial demonstrate the ability of the ZIF-8/GOx&HRP *in-situ* biosensor to withstand high temperature conditions. Although in practical cases, the surrounding temperature will not reach as high as 100 ^{o}C, this temperature is used to test the robustness of ZIF-8/GOx&HRP *in-situ* against thermal degradation. Lastly, experiments of stability against inhibitor will suggest the type of ZIF-8 structure surrounding the enzymes in ZIF-8/GOx&HRP *in-situ* composites.

Acid stability: The result shows that the performance of ZIF-8/GOx&HRP *in-situ* patterning in pH 5 has slightly reduced compared to the control samples in pH 7.4 (**Figure 4a**). ZIF-8/biomolecules composites stability test in low pH condition has been well-studied in various literature [2, 51-52], in which, the degradation of ZIF-8 in acidic condition is measured by the intensity of fluorescence or amount of biomolecules released from ZIF-8 matrix. Generally long incubation time is needed to completely etch ZIF-8; for instance, 6 hours incubation in pH 6 results in approximately 90 % release of biomolecules.[2, 51]

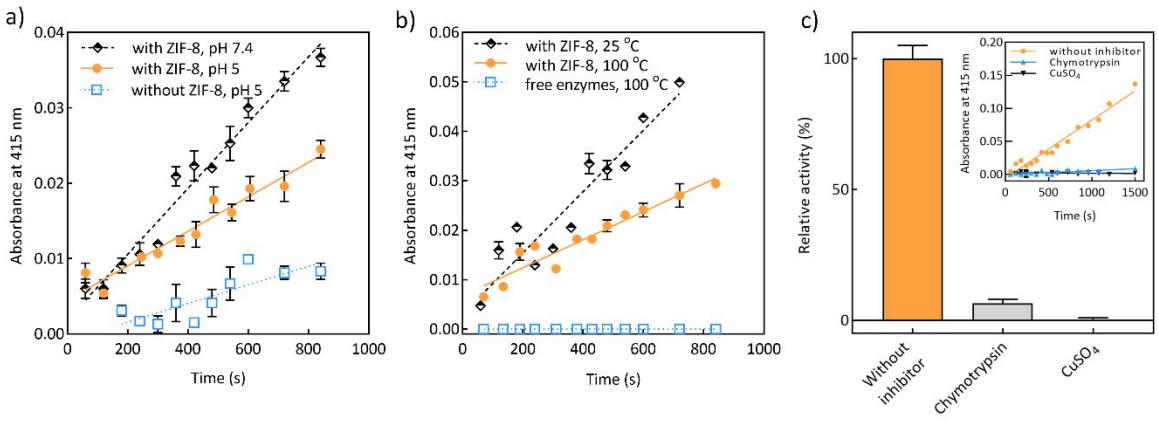

Figure 4. a) Absorbance value over time of bio-composites with and without ZIF-8 performance in acidic condition (pH 5) compare with control (with ZIF-8, pH 7.4); b) Performance of bio-composites with ZIF-8 after incubation in 100 °C of water for 1 hour, no residual activity of free enzyme with the same treatment, compared with control (with ZIF-8, 25 °C); c) Relative activity of ZIF-8/GOx&HRP *in-situ* after incubation in various inhibitors (Chymotrypsin and $CuSO_4$) for 30 minutes with insert showing absorbance value over time of bio-composites with ZIF-8 (ZIF-8/GOx&HRP *in-situ*) performance after incubation in Chymotrypsin and $CuSO_4$.

In our study, the incubation of ZIF-8/GOx&HRP *in-situ* thin film in pH 5 is conducted for 30 minutes which is 3 times longer than the required sensor time of 10 minutes, when used with physiological fluid. When compared with control condition of pH 7.4, the enzyme activity has slightly decreased. This finding is consistent with the study by Tian et al.,[52] whom reported that ~20 % and ~40% drug are released at pH 6 and pH 4.5 respectively within 30 minutes; hence, we can expect that the ZIF-8/GOx&HRP thin film activity in pH 5 to be reduced to an extent.

To further support this explanation, a simple acid test was conducted with ZIF-8 particles at pH 5 to study the morphology of the particles before and after acid treatment, which shows the particles are slightly degraded; however, not completely dissolved after an incubation time of 30 minutes, as shown in **Figure S10.** In a broader context, the acid test proved that ZIF-8 has a potential application in controlled release of protein in drug delivery by utilizing the increased in enzyme loading and disintegration mechanism for drug release in low pH microenvironment.

Nonetheless, it is worth to note that the ZIF-8/GOx&HRP *in-situ* shows a higher activity than the samples without ZIF-8 at pH 5 condition (**Figure 4a**). The higher activity of ZIF-8/GOx&HRP *in-situ* can also be explained by disintegration of ZIF-8 in pH 5,[53] through the breaking of the coordination bond between zinc centers and imidazolate ligands.[54] Since ZIF-8/GOx&HRP *in-situ* has higher enzymatic loading than sample without ZIF-8 (refer to ICP-MS results); the acid will expose more enzymatic active sites for reactions; thus, serves as an indirect evidence for biomineralization of the enzymes on the surface of PDA/PEI patterning.

Although the device does shows lower activity in acidic condition compared to normal condition, this area allows more room for improvement and further research. Indeed, the significant increase in stability of the device compared with the device without ZIF-8 should be emphasized to establish the role of ZIF-8 in this device.

Thermal stability: When subjected to 100 ^{o}C boiling water for 1 hour; the ZIF-8/GOx&HRP *in-situ* shows slightly decreased activity when compared to the performance of the device in control condition at 25 ^{o}C (**Figure 4b**). Nonetheless, the role of ZIF-8 in increasing the thermal stability of the enzyme is apparent as there are no detectable activity from the free enzyme after heat treatment of 100 ^{o}C. These results corroborates with previous finding in literature,[2] suggesting that the *in-situ* biomineralization protects the tertiary and quaternary structure of the enzyme from thermal degradation.

Inhibitor stability: Lastly, we studied the effect of introducing known enzyme inhibitor such as chymotrypsin and copper (II) sulfate ($CuSO_4$). Chymotrypsin which is a digestive enzyme that cleaves peptides (protein primary structures) at hydrophobic residues, has a similar tertiary structure with trypsin.[55] Therefore, chymotrypsin was used in this experiment as an analog to digestive enzyme trypsin which was predominantly used in previous literature to exhibit ZIF-8 protective properties.[2, 7] Copper (II) ions (Cu^{2+}) was

known to severely inhibit GOx,[56-57] and due to its susceptibility to Cu^{2+}, GOx has been studied for its potential to be used of Cu^{2+} detection.[57] Based on our results, there is a significant reduction in the activity of the ZIF-8/GOx&HRP *in-situ* patterns when pre-treated with enzyme inhibitors for 30 minutes (**Figure 4c**). As expected, there is no residual activity observed when the samples are pre-treated with $CuSO_4$ (pH 8.83) as ZIF-8 structure can be penetrated by Cu^{2+} as shown in previous literature;[58] hence, enabling inhibition of the enzyme active sites. Interestingly, the activity of ZIF-8/GOx&HRP *in-situ* patterns declines significantly to 6.67 ± 1.38 % when pre-treated with chymotrypsin. Considering the size of chymotrypsin is of larger magnitude than ZIF-8 pores, this suggests that the encapsulated GOx and HRP are partially exposed to the surface of the thin films or alternatively, there are passageways within the thin film that enable chymotrypsin to access the encapsulated enzymes.

In summary, the thermal and chemical stability of ZIF-8/GOx&HRP *in-situ* composites indicates that the structural conformation of the enzyme can be preserved in the enzyme-MOF thin film. In other words, in elevated temperatures and low pH conditions, the unfolding of proteins which corresponds to the disruption of tertiary and quaternary structure of protein will occur. As the result shows enhanced thermal and pH stability, this leads us to deduce that the ZIF-8 film stabilizes the tertiary and quaternary structural conformation of the enzyme by acting as "tether" and hold the enzyme in confinement. Besides that, the low inhibitor stability by chymotrypsin experiment alluded that the ZIF-8/GOx&HRP *in-situ* cannot prevent the cleaving of secondary structure (peptide bonds) to amino acids and the small Cu^{2+} ions can alter the active site of the enzyme, subsequently changing the enzyme's inner structure. These experimental results are in agreement with a previous study by Liao et al. [8] which has demonstrated that the sodalite structure (SOD) of ZIF can provide enzyme structural conformational stability from unfolding element (temperature and pH) while still

can be affected by infiltration of active site inhibitors. Hence, the mechanism of enzyme protection from environment conditions (high temperature, low pH and presence of inhibitors) in enzyme-MOF thin films and enzyme-MOF particles can be different.

Spatial location of the enzyme: Based on the inhibitor stability results, we can postulate the location of the enzyme GOx&HRP in the ZIF-8 thin films. There are three cases that can be considered which are Case I: enzyme underneath MOF, Case II: enzyme partially exposed to the surface and Case III: fully encapsulated enzyme within the matrices which are illustrated in **Figure 5 a, b, and c** respectively. It is expected that the scattering of enzymes underneath the MOF crystals (Case I) will pose mass transfer issues as the movement of substrate will be limited. In Case II, the exposed enzymes to the surface will increase the enzyme susceptibility to inhibitors and chelating agents. Lastly, in Case III, the enzyme will be protected and encapsulated within the MOF thin films.

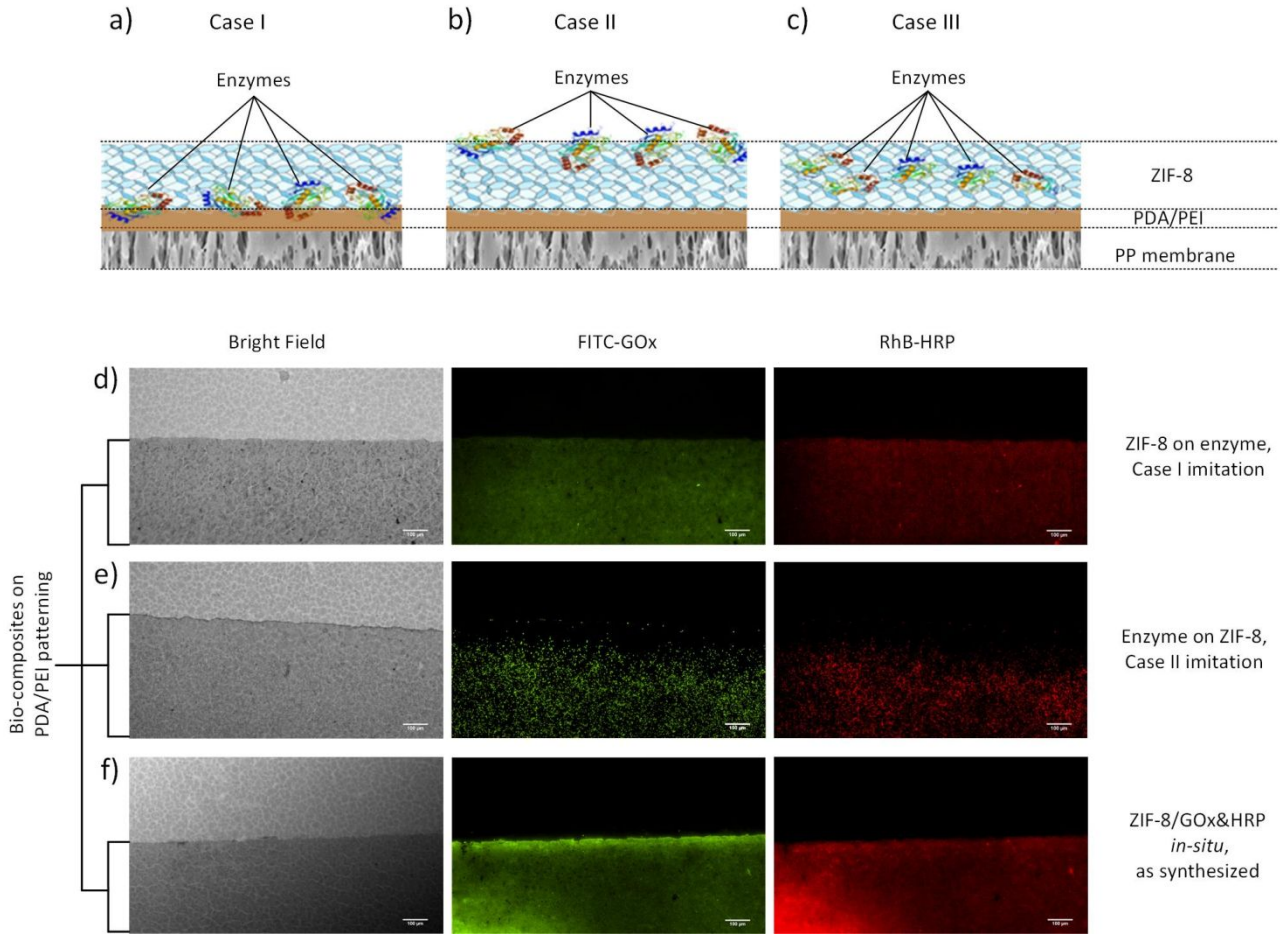

Figure 5. Schematic illustration of a) Case I; b) Case II; c) Case III; and fluorescence microscopy images in bright field mode and fluorescence mode of FITC-GOx and RhB-HRP with different location of enzymes in sample such as d) Case I imitation, the enzymes are beneath the ZIF-8 layer; e) Case II imitation, the enzyme are on top of ZIF-8 layer; and finally, f) our ZIF-8/GOx&HRP *in-situ* sample, as synthesized. Scale bar is 100 μm long in all images.

We infer that Case I does not represent the spatial enzyme distribution in ZIF-8/GOx&HRP *in-situ* since it has higher enzyme loading compared to sample with PDA/PEI-GOx&HRP, based on the ICP-MS results. The higher loading of the enzyme in ZIF-8/GOx&HRP *in-situ* was attributed to biomineralization where some of the enzymes will be encapsulated within the ZIF-8 matrices compared to enzymes deposited on the surface of PDA/PEI without the presence of ZIF-8. From the chymotrypsin inhibitor test, it is obvious that the enzymes are severely impacted by the presence of inhibitors which lead to initial deduction that the enzymes are not fully encapsulated within the matrix of ZIF-8 as depicted in Case III; hence, the combination of Case II and Case III is more likely to represent the spatial location of enzyme in ZIF-8/GOx&HRP *in-situ* thin film.

To assess this hypothesis, a fluorescence microscopy test was performed to qualitatively analyze the location of the enzymes in the patterns. Bio-composite patterning of Case I employed a layer of enzyme on top of PDA/PEI patterns with ZIF-8 thin film growth on top (layer-by-layer) and Case II with enzyme immobilized on top of ZIF-8 thin film was developed to be compared with ZIF-8/GOx&HRP *in-situ*. In each sample, fluorescence labelled enzymes such as fluorescein isothiocyanate-glucose oxidase (FITC-GOx) and rhodamine B-horseradish peroxidase (RhB-HRP) are used. Note that the optical microscope views the 2-D images of the samples from the top view.

The fluorescence emission photographs of the samples are as in **Figure 5 d-f**. **Figure 5d** shows when the enzymes are beneath the ZIF-8 structure, the fluorescence emissions are more evenly dispersed, and the emission intensity is dampened. On the other hand, **Figure 5e** shows sparsely distributed enzymes with high intensity emissions when the enzymes are

deposited on top of the ZIF-8 structure. Comparison of these two figures shows that the different spatial arrangement of enzymes can be observed with fluorescence microscopy images. Next, we observe the fluorescence images of the ZIF-8/GOx&HRP *in-situ* as synthesized (**Figure 5f**) which indicates that the enzymes are biomineralized within the ZIF-8 matrix based on the even dispersion of the enzyme fluorescence emissions; and the high intensity indicates that the enzymes might be closer to the surface. This arrangement resembles a combination of Case II and Case III as proposed and supports the findings from the chemical, thermal and stability test.

In the future, using more sophisticated characterization methods such as super-resolution fluorescence microscopy might offer 3-D view of the spatial location of the enzyme in the ZIF-8 matrix. Nonetheless, the preliminary fluorescence microscopy images combined with stability results are satisfactory to suggest that the spatial enzyme distribution in the enzyme-MOF thin film structure is different than the enzyme-MOF particles.

2.4. Biosensor Performance Evaluation

To evaluate the performance of ZIF-8/GOx&HRP *in-situ* thin films as glucose biosensor, the selectivity towards glucose against interference of other analytes and the sensitivity of the biosensor to provide a linear response range are studied. In this study, the sensitivity of ZIF-8/GOx&HRP *in-situ* is calculated as response (absorbance value) over concentration of glucose. Next, the Limit of Detection (LoD) to determine the lowest concentration of glucose that reliably produce a response and the ability of the ZIF-8/GOx&HRP *in-situ* to produce a readout scheme for eye-detection will be evaluated as biosensor performance criteria.

2.4.1. Selectivity

The ZIF-8/GOx&HRP *in-situ* thin film biosensor shows high selectivity towards glucose in comparison with other type of carbohydrates and interferences (albumin, lactose, sucrose and glycogen) when tested within 10 minutes (**Figure 6a**). This result is comparable with ZIF-8/GOx&HRP composite particles in the literature.[7]

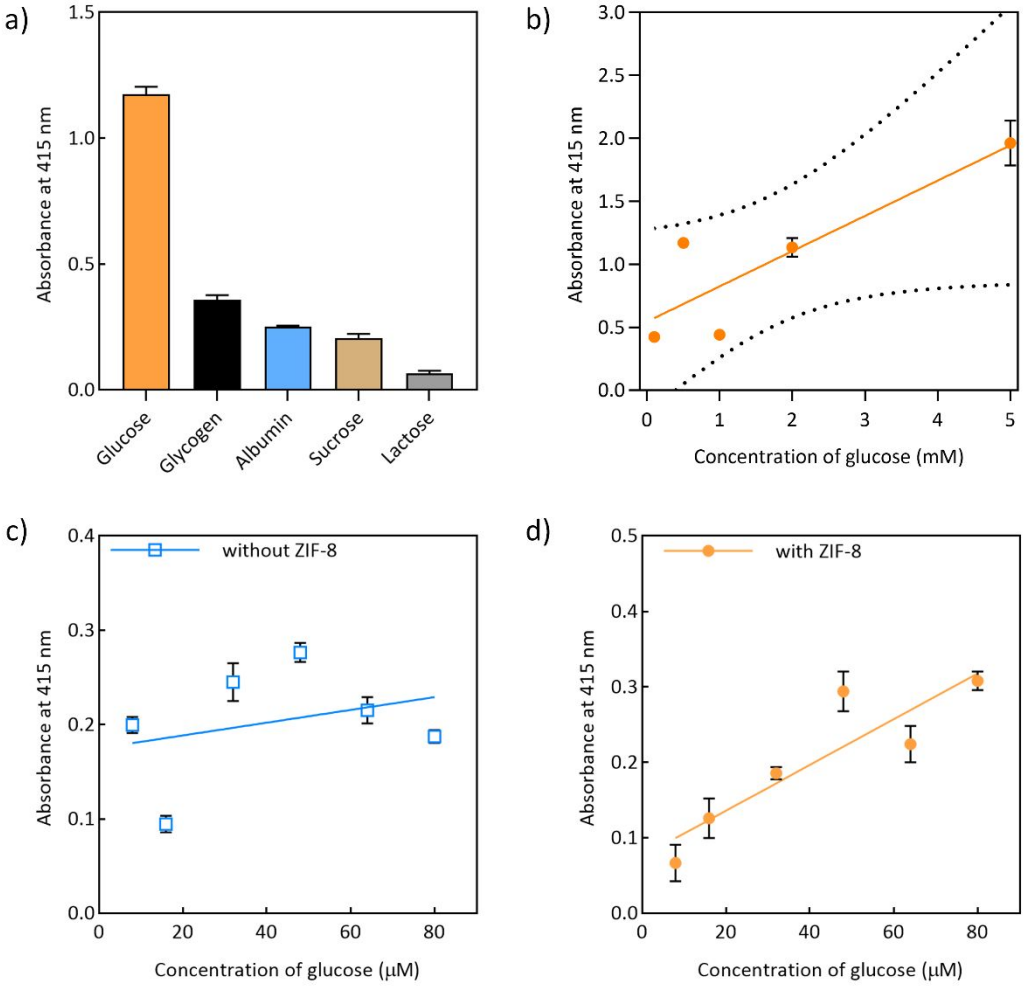

Figure 6. a) Selectivity test of the ZIF-8/GOx&HRP *in-situ* using 1 mM of glucose, 1 mg/mL of albumin, 1 mM of lactose, 1 mM of sucrose and 1 mM of glycogen; b) sensitivity test of ZIF-8/GOx&HRP *in-situ* with glucose concentration in mM range shows linear span of concentration of glucose until ~ 5 mM; c) sensitivity test of PP-PDA/PEI-GOx&HRP (without ZIF-8) and d) sensitivity test of ZIF-8/GOx&HRP *in-situ* (with ZIF-8) with concentration of glucose of 8, 16, 32, 48, 60 and 80 μM.

2.4.2. Sensitivity

The ZIF-8/GOx&HRP *in-situ* shows linear sensitivity when tested in low concentration range of glucose (8, 16, 32, 48, 64 and 80 μM). The ZIF-8/GOx&HRP *in-situ* strips (**Figure 6d**) has higher sensitivity of 0.00303 Abs/μM compared to the strips without ZIF-8 (PP-PDA/PEI-GOx&HRP only) 0.00068 Abs/μM (**Figure 6c**).

In practice, a reliable sensor device should exhibit a linear relationship over a wide span of analytes concentration. The deviation from linearity is a common problem in different type of sensors which is well-explained in the review paper by Mross et al.[31] The limiting key factor of enzyme linear kinetic is the Michaelis -Menten constant (K_m), which quantifies the affinity of the substrate (S) to the enzyme (E); forming an enzyme-substrate (ES) complex.[31] Well below K_m, the reaction rate increases linearly, until it reaches a point whereas the saturation of substrate molecules on the surface of the enzyme (ES formation) which reduces the available oxygen for the enzyme oxidase reactions.[31] Due to the oxygen scarcity, the ES complex is unable to return to its original E form for the next conversion. [31]

Several measurements were proposed by Mross et al. to extend the linear measurement range; such as employing diffusion limiting membrane, using redox mediator for oxygen replenishment and substrate dilution using controlled flow in microfluidic channels.[31] Based on the initial results of the sensitivity test, we propose ZIF-8/GOx&HRP *in-situ* thin film to provide a diffusion limiting effect; hence, resulting in high linear sensitivity for signal measurement at wider range of substrates concentration (from very low to very high concentration).

The concentration of glucose in bodily fluid for normal and diabetic patients were summarised by Bruen et al.;[33] ranging from 0.01 mM of glucose in sweat, up to 40 mM of glucose in the blood.[33] This warrants an extended investigation for the sensitivity test of ZIF-8/GOx&HRP *in-situ* at higher concentration of glucose. Therefore, three sets of repeat

experiments were done for the glucose concentration of 1, 2, 5, 8, 10, 20, 30 and 40 mM; and the readings were taken after 10 minutes of reaction. Note that these concentrations are at 1000 times higher than the previous test which was in the μM range (**Figure S11**). **Figure S11** shows that the absorbance increases as the concentration of glucose increases from 1 to 5 mM and started to exhibit a decline in trend for concentrations higher than 10 mM showing substrate inhibition behaviour. The substrate inhibition is confirmed for the ZIF-8/GOx&HRP *in-situ* as explained earlier; however, it occurs at a higher limit of concentration range ~5 mM. Therefore, the linear span of ZIF-8/GOx&HRP *in-situ* ranges from 8 μM to 5 mM.

It is claimed that the linear sensitivity is observed at low concentration range of glucose concentration within micromolar concentration range, and when extended to millimolar concentration range, the linear trend is also exhibited. While the linearity is maintained, the sensitivity (slope) changes accordingly due to the difference in the resolution of measurement. At higher concentration range of glucose, the sensitivity is reported to be 0.2798 Abs/mM (**Figure 6b**). Since the data point in millimolar concentration range are further apart than in the micromolar range, the sensitivity decreases in one order of magnitude due to difference in the resolution of the test.

2.4.3. Detection limits

In this work, the Limit of Blank (LoB) and Limit of Detection (LOD) will be calculated to determine the smallest concentration of analyte [59] that can be reliably detected using the MOF-based enzymatic biosensor using Cary 300 UV-Vis spectrometer at 415 nm. LoB is defined as the highest value measured when repeated of blank samples containing no analytes are done.[59] In our case, the LoB was done by measuring the absorbance value of blank sample without the converted ABTS radicals (conversion of glucose was not initiated); thus, acquiring the mean ($mean_{blank}$) and standard deviation (SD_{blank}).[59] The LoB was calculated using $LoB = mean_{blank} + 1.645(SD_{blank})$.[59] LoD is defined at the lowest concentration of analyte that can be detected by the measured protocol, with the equation of $LoD = LoB + 1.645(SD_{low\ concentration\ sample})$; in which $SD_{low\ concentration\ sample}$ is the standard deviation of samples with low concentration of analytes. When using this statistical method, it is understood that at least 95% of the low concentration samples will lie above the defined LoB; validating the LoD as the lowest possible concentration of analyte that can be detected.

The LoD was found to be 0.0027 value of absorbance at 8 μM concentration of glucose and the LoB was calculated to be at 0.0005 absorbance value. All 11 individual tests with 8 μM concentration of glucose results in absorbance values above LoB; thus, validating the LoD at 8 μM glucose concentration.

2.4.4 Comparison of performance with glucose biosensors

The sensitivity, LoD and linear span of the thin film ZIF-8/GOx&HRP *in-situ* are of comparable performance to other particulate colorimetric glucose biosensors in past literatures (**Table 1** and **Figure 7**).[7, 60-65] The performance of ZIF-8/GOx&HRP *in-situ* is superior in terms of linear span compared to ZIF-8/GOx&HRP composites in free particle systems.[7] It is worth to note that the sensitivity of ZIF-8/GOx&HRP *in-situ* thin film is lower than ZIF-8/GOx&HRP in particle form[7] due to the suspended free particle systems allowing higher surface area for enzymatic reaction. Nonetheless, the thin film form is more desirable as a portable point of care device, as further separations of nanoparticles from the solution are not required.

The concept of nanoparticle-sensors separation using magnetic field has led to the synthesis of magnetic ZIF-8 and glucose oxidase composites (mZIF-8@GOx) for glucose sensing purposes.[62] The ZIF-8/GOx&HRP *in-situ* thin film is of commensurate sensitivity with mZIF-8@GOx (reported sensitivity 0.00309 Abs/μM); with the benefit of eliminating the need to perform a separation process.[62] Compared to other nano-materials such as carboxylic acid functionalized graphene oxide[60] and cobalt (II,III) oxide nanoparticles;[61] ZIF-8/GOx&HRP *in-situ* bio composites possess greater performance in terms of sensitivity. Lastly, the LoD of ZIF-8/GOx&HRP *in-situ* is relatively low while still maintaining wide linearity when compared with optical detector,[64] microfluidic systems[63] and microfluidic paper-based devices[65] for glucose biosensing purposes.

Table 1. Comparison of ZIF-8/GOx&HRP *in-situ* biosensor performance with enzyme-based glucose biosensor in literature, in terms of sensitivity, limit of detection (LoD) and linear span.

Label	Sensitivity[a] (Abs/μM)	LoD[b] (μM)	Linear Span[c]	Description	Ref.[d]
A	0.00303	8	8 μM to 5 mM	ZIF-8/GOx&HRP in-situ thin film; cascades of reaction	This work
B	0.00820	0.5	8 μM to 64 μM	ZIF-8/GOx&HRP particles; cascades of reaction	7
C	0.00076	1	1 μM to 2 μM	GOx and Graphene Oxide-COOH[e]; free system; cascades of reaction	60
D	0.00011	5	10 μM to 10 mM	GOx, Co_3O_4[f] nanoparticles; free system; cascades of reaction	61
E	0.00309	1.9	5 to 150 μM	mZIF-8[g]@GOx nanoparticles; free system	62
F	0.00003	260	Up to 5 mM	Silica- PEG[h]-GOx&HRP; microfluidics	63
G	Not reported	23.8	0.1 to 2.5 mM	PB*i*–GOx–PEDD[j]	64
H	Not reported	300	Up to 10 mM	μPAD[k] biosensor; paper-based	65

[a] Sensitivity: The slope of calibration graph, (Absorbance / concentration of glucose (μM)). [b] Limit of detection (LoD): Lowest concentration of analyte that can be detected (μM). [c] Linear span: The range of analyte concentration for linear measurement. [d] References. [e] -COOH: carboxylic acid functional group. [f] Co_3O_4: cobalt (II,III) oxide. [g] mZIF-8: magnetic ZIF-8. [h] PEG: polyethylene glycol. [i] PB: Prussian Blue. [j] PEDD: paired emitter-detector diodes. [k] μPAD: microfluidics paper based analytical devices.

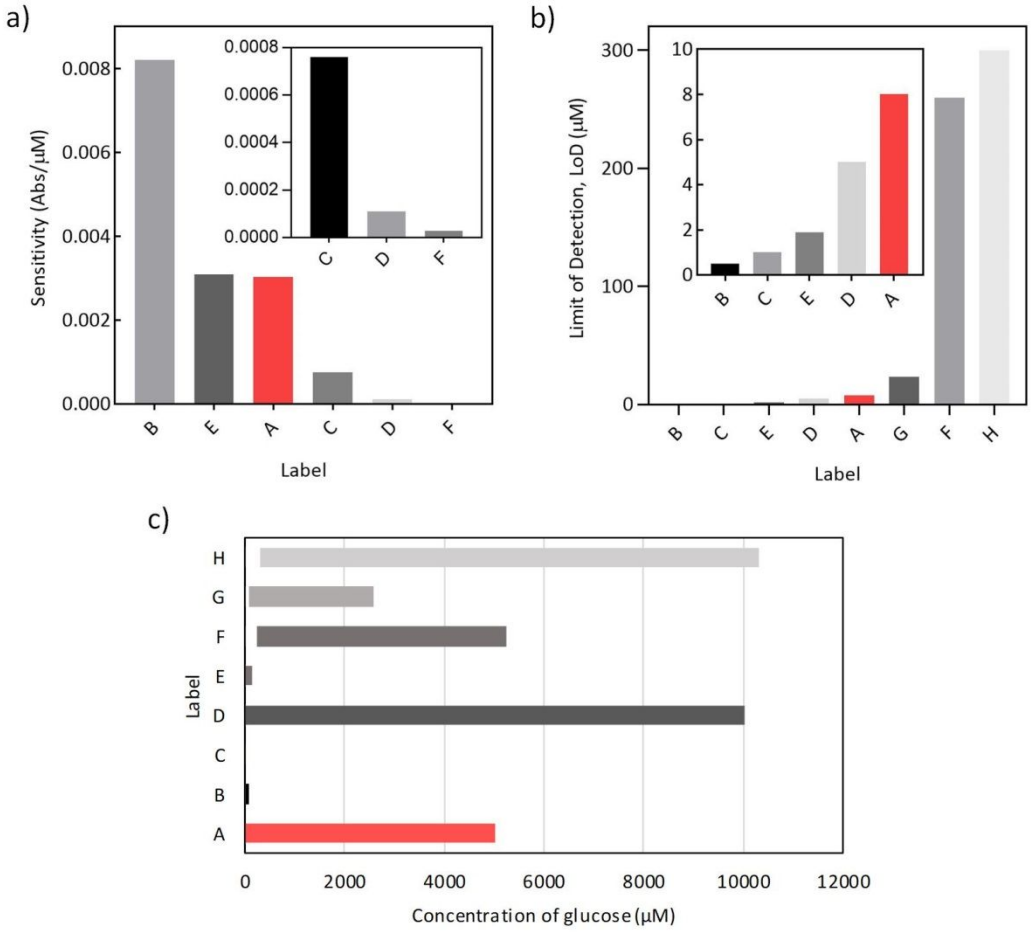

Figure 7. ZIF-8/GOx&HRP *in-situ* biosensor performance (Label A, red bar) in terms of a) sensitivity, (Abs/µM); b) Limit of Detection, LoD (µM) and c) linear span (µM); in comparison with glucose sensors from literature; labelled B-H, as referenced in **Table 1**.

In summary, the performance of ZIF-8/GOx&HRP *in-situ* is outstanding considering the added advantage of ease of handling of thin-films to be used in devices, compared to other new materials in free particles system.[7, 60-65] With further optimization, the biosensor performance can be improved. When combined with good thermal and acid stability; ZIF-8/GOx&HRP *in-situ* is definitely a competitive alternative synthesis method for the conventional paper-based biosensor.

2.4.5. Readout Schemes for Glucose Sensing Application

One of the applications of ZIF-8/GOx&HRP patterns is to be used as a testing strips for visible detection of glucose; providing an indicator of ranges of glucose analytes concentration in the sample. In **Figure 8a**, the readout scheme shows visible detection limit of 0.5 mM which is comparable with the readout schemes from existing studies by Wu et al.[7] using ZIF-8/GOx&HRP particles on paper strips with the same duration of response time (t=10 mins). At the concentration of 0.1 mM, the color change after 10 minutes incubation time is barely visible. The range of readout scheme from 0.5 mM to 8 mM is suitable to be used for glucose detection using ocular fluid and saliva of diabetic patients with glucose concentration of 0.5-5 mM and 0.55-1.77 mM respectively.[33]

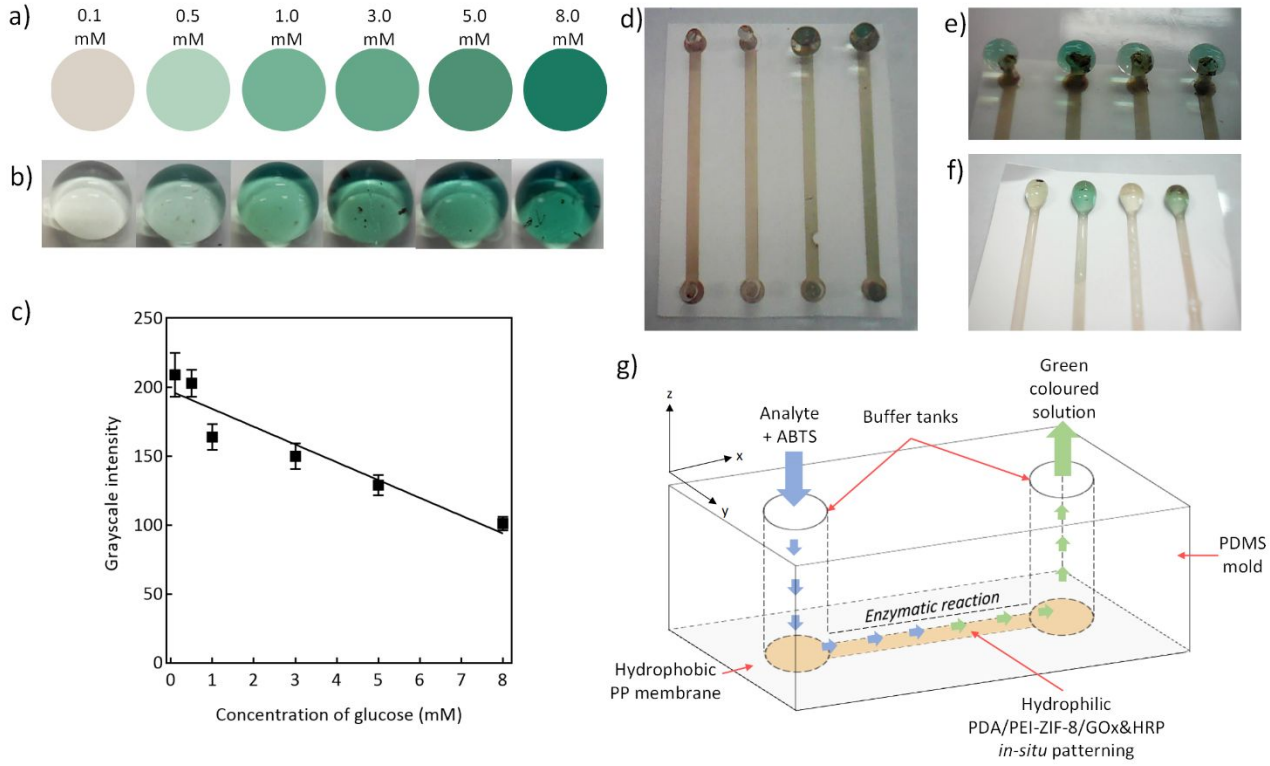

Figure 8. a) Proposed readout scheme for glucose concentration ranges from 0.1 to 8.0 mM with detection limit of 0.5 mM; with b) corresponding images of droplets at the respective concentration; c) grayscale intensity of droplets images against concentration of glucose (mM) d) demonstration of color change in microfluidic channels (2 from right with glucose analytes); e) photograph of colored response from testing strips in microfluidic channels for solution with the same concentration of glucose; f) photograph of colored response from testing strips without microfluidic channels, with different concentration of glucose; and g)

schematic drawing of PDMS microfluidic channels containing the fluid on hydrophilic patterning, for enzymatic reaction to occur (figure drawn not in scale).

Practical considerations in applying the readout schemes are the response time, the volume of analytes and the enzyme loading capacity in each of the testing strips. This is because, a variance in one of the parameters will affect the final color of the solution. For instance, a longer incubation time, lower volume of analyte and higher enzyme loading capacity will results in solution with higher intensity of color change. Nonetheless, the first two parameters can be controlled by integrating the testing strips systems with a timing and optical device for increased accuracy. The enzyme loading can only be controlled during manufacturing steps; thus, any discrepancy should be recognized as a systematic error. Whilst accuracy of glucose monitoring is not the main aim of using bare eye for optical detection; the ZIF-8/GOx&HRP patterning does provide a fast method to determine a concentration range of glucose analytes in a sample, based on the readout scheme.

In the future, paired usage of the glucose testing strips with handheld optical sensing device (e.g. smartphone with downloadable applications) can be developed.[65] To demonstrate the detection ability by optical devices, the grayscale intensity was calculated from the RGB color scale of the droplet images. The result shows that the grayscale intensity has an inversely proportional relationship to the concentration of glucose (**Figure 8c**); indicating the feasibility of the optical device sensing strategy with the ZIF-8/GOx&HRP glucose sensing strips.

3. Conclusions

In conclusion, a facile two-step fabrication of hydrophilic patterning and enzyme-MOF thin film for enzyme-based biosensor application has been demonstrated in this paper; and the characteristic, stability and performance of the biosensor were investigated. We utilized a unique patterning method of PDA/PEI on hydrophobic PP membrane with microfluidic structure which provides liquid pumpless transportation. This method is cost-effective and increases the device flexibility for onsite applications. Next, the enzyme GOx and HRP and MOF ZIF-8 were used as a proof of concept for simultaneous nucleation and growth of ZIF-8/GOx&HRP thin film on the PDA/PEI patterning. The ZIF-8 structure is confirmed on the patterns; with higher density of ZIF-8 when enzyme is added. The acid and thermal stability test shows that the enzyme structure is preserved in the ZIF-8/GOx&HRP *in-situ*; however, the susceptibility of the composite to inhibitors suggests that further studies are required to confirm the spatial arrangement of enzyme in the ZIF-8 matrix and its effects. The biosensor performance of ZIF-8/GOx&HRP *in-situ* shows a good selectivity, high sensitivity, sufficient LoD and linear response in a wide span range that is comparable with other sensors based on new materials in the literature. The sensitivity result indicates that the ZIF-8 structure in ZIF-8/GOx&HRP *in-situ* can contribute to the linear sensitivity by providing a diffusion limiting effect, compared to samples without ZIF-8. Overall, this study has demonstrated a universal approach in utilizing enzyme-MOF thin film as a biosensor whereby the application can be extended to other enzyme cascades such as amylase-GOx&HRP for starch detection.

4. Experimental Section

Reagents and Chemicals: All reagents and chemicals used were purchased from Sigma-Aldrich, otherwise specified; at highest purity and used without further purification. All experiments were performed in room temperature and pressure unless stated otherwise. Milli-Q® water dispensed from Milli-Q® IQ 7000 Ultrapure Lab Water System (Merck Millipore) is used for buffer preparation.

Microfluidic structure preparation: There were two main steps involved in preparing the PDMS mold. The first step was to create the silicon wafer master template with the negative photoresist SU-8 bumps. The 4" silicon wafer (TED-PELLA, Resistivity 1-100 ohm cm^{-1}, Orientation: <100>) was pre-treated with isopropanol and acetone prior to the spin coating of SU-8 onto the silicon wafer at 1500 rpm for 30 s. Afterwards, the wafer was baked at 100 ^{o}C for 50 s. The SU-8 patterning of microchannels was achieved *via* negative photolithography technique, which requires the transfer of microchannels geometrical shapes from a negative mask *via* exposure of the UV light for 3.5 s. The photolithography process was followed by developing process and final rinse with isopropanol. The final dimension of the SU-8 bumps are 1 mm wide with 20 μm height. Once the master template was obtained, the PDMS mold was prepared by pouring the PDMS mixture of 9:1 parts of silicone:hardener (Sylgard® 184 silicone elastomer kit) onto the master template. The air bubbles in the PDMS mixture was removed in the vacuum oven at room temperature before being cured at 78 ^{o}C for 40 minutes.

PDA/PEI patterning: Dopamine hydrochloride (2 mg mL^{-1}) and polyethyleneimine (PEI) (2 mg mL^{-1}) was prepared in Tris-HCl buffer solution (0.05 M, pH 8.5) with 10 v/v % of ethanol (100 %, denatured). It is recommended to add the dopamine hydrochloride prior to patterning to prevent premature polymerization of polydopamine. This mixture was injected into the microfluidic channels on polypropylene membrane (hydrophobic, Accurel® PP 2E

HF (R/P) from Membrana GmBH) to develop patterns for 4 hours. Then, the patterns were rinsed with Milli-Q® water.

ZIF-8 thin film synthesis (control): ZIF-8 precursor solution (5 mL) was prepared from precursors which are zinc nitrate hexahydrate, $Zn(NO_3)_2.6H_2O$ (0.0135 g) and 2-methyl imidazole, HMIM (0.2830 g). The solution was injected into the microfluidic channels with PDA/PEI pattern to allow ZIF-8 growth. After 30 minutes, the patterns in the channels were rinsed with Milli-Q® water.

ZIF-8/GOx&HRP in-situ thin film synthesis: Enzyme solution (0.4 mL, 5 mg mL^{-1} GOx, 7.5 mg mL^{-1} HRP) was mixed with ZIF-8 precursor solution (5 mL, 0.0135 g $Zn(NO_3)_2.6H_2O$, 0.2830 g HMIM). The solution turned cloudy with the presence of enzyme solution which indicates that the nucleation of ZIF-8 was accelerated. The solution was then immediately pipetted into the microchannel to be deposited on the PDA/PEI coating for 30 minutes; followed by Milli-Q® water rinse.

Detailed instrumentation and experimental methods are included in the **Supporting Information (SI) Document**.

ASSOCIATED CONTENT

Supporting Information

Supporting Information is available free of charge via the Internet at http://pubs.acs.org.

1) Details of experimental sections including instrumentation, selectivity test, sensitivity test, acid stability test, thermal stability test, inhibition stability test, enzyme labelling protocol for fluorescence microscopy, activity comparison of different immobilization strategies of enzyme-MOF onto the PDA/PEI patterning *via* ZIF-8/GOx&HRP *in-situ* thin film, SEM images of ZIF-8 thin films on PDA/PEI coated PP membranes with ZIF-8 and ZIF-8/GOx&HRP nucleation times of 5, 10, 15, 20, 25 and 30 minutes respectively, 2-D AFM height sensor images with respective 3-D images inserts, detailed stacked FT-IR spectra, detailed overlapped TGA results, detailed XRD patterns, substrate inhibition behavior of the device and table of RGB values of droplet images. (Portable Document Format, PDF, .pdf)

2) Video of pumpless transportation demonstration by the hydrophilic PDA/PEI patterning on the hydrophobic PP membrane. (QuickTime, .mov)

AUTHOR INFORMATION
Corresponding Authors
* Dr. Amir Razmjou, email: amirr@unsw.edu.au
* Prof. Vicki Chen, email: v.chen@uq.edu.au

ORCID
Amir Razmjou: 0000-0002-3554-5129

Present Address
†UNESCO Centre for Membrane Science and Technology, School of Chemical Engineering, University of New South Wales, Sydney 2052, Australia

Funding
Australian Research Council's Discovery Projects funding scheme (DP150104485 and DP180103874)

ACKNOWLEDGEMENT
The authors would like to acknowledge the financial support from Australian Research Council's Discovery Projects funding scheme (DP150104485 and DP180103874). The authors acknowledge the use of facilities supported by AMMRF at the Electron Microscope Unit at UNSW.

TOC FIGURES / GRAPHICAL ABSTRACT

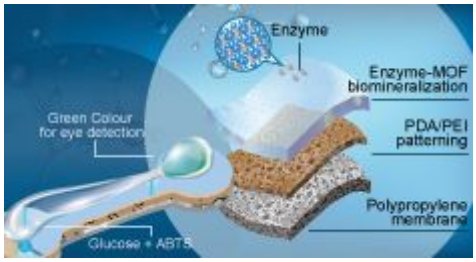

REFERENCES

(1) Luka, G.; Ahmadi, A.; Najjaran, H.; Alocilja, E.; DeRosa, M.; Wolthers, K.; Malki, A.; Aziz, H.; Althani, A.; Hoorfar, M. Microfluidics Integrated Biosensors: A Leading Technology towards Lab-on-a-Chip and Sensing Applications. *Sensors (Basel, Switzerland)* **2015,** *15* (12), 30011-30031, DOI: 10.3390/s151229783.

(2) Liang, K.; Ricco, R.; Doherty, C. M.; Styles, M. J.; Bell, S.; Kirby, N.; Mudie, S.; Haylock, D.; Hill, A. J.; Doonan, C. J.; Falcaro, P. Biomimetic mineralization of metal-organic frameworks as protective coatings for biomacromolecules. *Nature Communications* **2015,** *6*, 7240, DOI: 10.1038/ncomms8240.

(3) Lyu, F.; Zhang, Y.; Zare, R. N.; Ge, J.; Liu, Z. One-Pot Synthesis of Protein-Embedded Metal–Organic Frameworks with Enhanced Biological Activities. *Nano Letters* **2014,** *14* (10), 5761-5765, DOI: 10.1021/nl5026419.

(4) Shieh, F.-K.; Wang, S.-C.; Yen, C.-I.; Wu, C.-C.; Dutta, S.; Chou, L.-Y.; Morabito, J. V.; Hu, P.; Hsu, M.-H.; Wu, K. C. W.; Tsung, C.-K. Imparting Functionality to Biocatalysts via Embedding Enzymes into Nanoporous Materials by a de Novo Approach: Size-Selective Sheltering of Catalase in Metal–Organic Framework Microcrystals. *Journal of the American Chemical Society* **2015,** *137* (13), 4276-4279, DOI: 10.1021/ja513058h.

(5) Gkaniatsou, E.; Sicard, C.; Ricoux, R.; Mahy, J.-P.; Steunou, N.; Serre, C. Metal-organic frameworks: a novel host platform for enzymatic catalysis and detection. *Materials Horizons* **2017,** *4* (1), 55-63, DOI: 10.1039/C6MH00312E.

(6) Lian, X.; Fang, Y.; Joseph, E.; Wang, Q.; Li, J.; Banerjee, S.; Lollar, C.; Wang, X.; Zhou, H.-C. Enzyme-MOF (metal-organic framework) composites. *Chemical Society Reviews* **2017,** *46* (11), 3386-3401, DOI: 10.1039/C7CS00058H.

(7) Wu, X.; Ge, J.; Yang, C.; Hou, M.; Liu, Z. Facile synthesis of multiple enzyme-containing metal-organic frameworks in a biomolecule-friendly environment. *Chemical Communications* **2015,** *51* (69), 13408-13411, DOI: 10.1039/C5CC05136C.

(8) Liao, F.-S.; Lo, W.-S.; Hsu, Y.-S.; Wu, C.-C.; Wang, S.-C.; Shieh, F.-K.; Morabito, J. V.; Chou, L.-Y.; Wu, K. C. W.; Tsung, C.-K. Shielding against Unfolding by Embedding Enzymes in Metal–Organic Frameworks via a de Novo Approach. *Journal of the American Chemical Society* **2017,** *139* (19), 6530-6533, DOI: 10.1021/jacs.7b01794.

(9) Liang, K.; Carbonell, C.; Styles, M. J.; Ricco, R.; Cui, J.; Richardson, J. J.; Maspoch, D.; Caruso, F.; Falcaro, P. Biomimetic Replication of Microscopic Metal–Organic Framework Patterns Using Printed Protein Patterns. *Advanced Materials* **2015,** *27* (45), 7293-7298, DOI: 10.1002/adma.201503167.

(10) Hou, M.; Zhao, H.; Feng, Y.; Ge, J. Synthesis of patterned enzyme–metal–organic framework composites by ink-jet printing. *Bioresources and Bioprocessing* **2017,** *4* (1), 40, DOI: 10.1186/s40643-017-0171-7.

(11) Shi, J.; Jiang, Y.; Zhang, S.; Yang, D.; Jiang, Z. Chapter Five - Biomimetic/Bioinspired Design of Enzyme@capsule Nano/Microsystems. In *Methods in Enzymology*; Challa Vijaya, K., Ed.; Academic Press: 2016; pp 87-112.

(12) Yang, H. C.; Waldman Ruben, Z.; Wu, M. B.; Hou, J.; Chen, L.; Darling Seth, B.; Xu, Z. K. Dopamine: Just the Right Medicine for Membranes. *Advanced Functional Materials* **2018,** *28* (8), 1705327, DOI: 10.1002/adfm.201705327.

(13) Yang, H.-C.; Hou, J.; Chen, V.; Xu, Z.-K. Surface and interface engineering for organic–inorganic composite membranes. *Journal of Materials Chemistry A* **2016,** *4* (25), 9716-9729, DOI: 10.1039/C6TA02844F.

(14) Gao, S.; Mohammad, M.; Yang, H.-C.; Xu, J.; Liang, K.; Hou, J.; Chen, V. Janus Reactors with Highly Efficient Enzymatic CO2 Nanocascade at Air–Liquid Interface. *ACS Applied Materials & Interfaces* **2017,** *9* (49), 42806-42815, DOI: 10.1021/acsami.7b14465.

(15) Tian, Y.; Cao, Y.; Wang, Y.; Yang, W.; Feng, J. Realizing Ultrahigh Modulus and High Strength of Macroscopic Graphene Oxide Papers Through Crosslinking of Mussel-Inspired Polymers. *Advanced Materials* **2013,** *25* (21), 2980-2983, DOI: 10.1002/adma.201300118.
(16) Yang, H.-C.; Xu, W.; Du, Y.; Wu, J.; Xu, Z.-K. Composite free-standing films of polydopamine/polyethyleneimine grown at the air/water interface. *RSC Advances* **2014,** *4* (85), 45415-45418, DOI: 10.1039/C4RA04549A.
(17) Hong, S.; Schaber, C. F.; Dening, K.; Appel, E.; Gorb, S. N.; Lee, H. Air/Water Interfacial Formation of Freestanding, Stimuli-Responsive, Self-Healing Catecholamine Janus-Faced Microfilms. *Advanced Materials* **2014,** *26* (45), 7581-7587, DOI: 10.1002/adma.201403259.
(18) Yang, H.-C.; Luo, J.; Lv, Y.; Shen, P.; Xu, Z.-K. Surface engineering of polymer membranes via mussel-inspired chemistry. *Journal of Membrane Science* **2015,** *483*, 42-59, DOI: 10.1016/j.memsci.2015.02.027.
(19) Shi, J.; Zhang, W.; Zhang, S.; Wang, X.; Jiang, Z. Synthesis of organic-inorganic hybrid microcapsules through in situ generation of an inorganic layer on an adhesive layer with mineralization-inducing capability. *Journal of Materials Chemistry B* **2015,** *3* (3), 465-474, DOI: 10.1039/C4TB01802H.
(20) Liu, Q.; Wang, N.; Caro, J.; Huang, A. Bio-Inspired Polydopamine: A Versatile and Powerful Platform for Covalent Synthesis of Molecular Sieve Membranes. *Journal of the American Chemical Society* **2013,** *135* (47), 17679-17682, DOI: 10.1021/ja4080562.
(21) Zhou, J.; Wang, P.; Wang, C.; Goh, Y. T.; Fang, Z.; Messersmith, P. B.; Duan, H. Versatile Core–Shell Nanoparticle@Metal–Organic Framework Nanohybrids: Exploiting Mussel-Inspired Polydopamine for Tailored Structural Integration. *ACS Nano* **2015,** *9* (7), 6951-6960, DOI: 10.1021/acsnano.5b01138.
(22) Wang, N.; Liu, Y.; Qiao, Z.; Diestel, L.; Zhou, J.; Huang, A.; Caro, J. Polydopamine-based synthesis of a zeolite imidazolate framework ZIF-100 membrane with high H2/CO2 selectivity. *Journal of Materials Chemistry A* **2015,** *3* (8), 4722-4728, DOI: 10.1039/C4TA06763K.
(23) Zhang, H.; Luo, J.; Li, S.; Wei, Y.; Wan, Y. Biocatalytic Membrane Based on Polydopamine Coating: A Platform for Studying Immobilization Mechanisms. *Langmuir* **2018,** *34* (8), 2585-2594, DOI: 10.1021/acs.langmuir.7b02860.
(24) Su, L.; Yu, Y.; Zhao, Y.; Liang, F.; Zhang, X. Strong Antibacterial Polydopamine Coatings Prepared by a Shaking-assisted Method. *Scientific Reports* **2016,** *6*, 24420, DOI: 10.1038/srep24420.
(25) Madhurakkat Perikamana, S. K.; Lee, J.; Lee, Y. B.; Shin, Y. M.; Lee, E. J.; Mikos, A. G.; Shin, H. Materials from Mussel-Inspired Chemistry for Cell and Tissue Engineering Applications. *Biomacromolecules* **2015,** *16* (9), 2541-2555, DOI: 10.1021/acs.biomac.5b00852.
(26) Liu, S.; Su, W.; Ding, X. A Review on Microfluidic Paper-Based Analytical Devices for Glucose Detection. *Sensors (Basel, Switzerland)* **2016,** *16* (12), 2086, DOI: 10.3390/s16122086.
(27) de Tarso Garcia, P.; Garcia Cardoso, T. M.; Garcia, C. D.; Carrilho, E.; Tomazelli Coltro, W. K. A handheld stamping process to fabricate microfluidic paper-based analytical devices with chemically modified surface for clinical assays. *RSC Advances* **2014,** *4* (71), 37637-37644, DOI: 10.1039/C4RA07112C.
(28) Cai, L.; Wang, Y.; Wu, Y.; Xu, C.; Zhong, M.; Lai, H.; Huang, J. Fabrication of a microfluidic paper-based analytical device by silanization of filter cellulose using a paper mask for glucose assay. *Analyst* **2014,** *139* (18), 4593-4598, DOI: 10.1039/C4AN00988F.
(29) Shirani, E.; Razmjou, A.; Tavassoli, H.; Landarani-Isfahani, A.; Rezaei, S.; Abbasi Kajani, A.; Asadnia, M.; Hou, J.; Ebrahimi Warkiani, M. Strategically Designing a Pumpless

Microfluidic Device on an "Inert" Polypropylene Substrate with Potential Application in Biosensing and Diagnostics. *Langmuir* **2017,** *33* (22), 5565-5576, DOI: 10.1021/acs.langmuir.7b00537.
(30) Kelly, M.; Macdougall, K.; Olabisi, O.; McGuire, N. In vivo response to polypropylene following implantation in animal models: a review of biocompatibility. *International Urogynecology Journal* **2017,** *28* (2), 171-180, DOI: 10.1007/s00192-016-3029-1.
(31) Mross, S.; Pierrat, S.; Zimmermann, T.; Kraft, M. Microfluidic enzymatic biosensing systems: A review. *Biosensors and Bioelectronics* **2015,** *70* (Supplement C), 376-391, DOI: 10.1016/j.bios.2015.03.049.
(32) Cho, N. H.; Shaw, J. E.; Karuranga, S.; Huang, Y.; da Rocha Fernandes, J. D.; Ohlrogge, A. W.; Malanda, B. IDF Diabetes Atlas: Global estimates of diabetes prevalence for 2017 and projections for 2045. *Diabetes Research and Clinical Practice* **2018,** *138*, 271-281, DOI: 10.1016/j.diabres.2018.02.023.
(33) Bruen, D.; Delaney, C.; Florea, L.; Diamond, D. Glucose Sensing for Diabetes Monitoring: Recent Developments. *Sensors* **2017,** *17* (8).
(34) Sperl, J. M.; Sieber, V. Multienzyme Cascade Reactions—Status and Recent Advances. *ACS Catalysis* **2018,** *8* (3), 2385-2396, DOI: 10.1021/acscatal.7b03440.
(35) Zhu, Z.; Kin Tam, T.; Sun, F.; You, C.; Percival Zhang, Y. H. A high-energy-density sugar biobattery based on a synthetic enzymatic pathway. *Nature Communications* **2014,** *5*, 3026, DOI: 10.1038/ncomms4026.
(36) Xia, S.; Zhao, X.; Frigo-Vaz, B.; Zheng, W.; Kim, J.; Wang, P. Cascade enzymatic reactions for efficient carbon sequestration. *Bioresource Technology* **2015,** *182*, 368-372, DOI: 10.1016/j.biortech.2015.01.093.
(37) Serra, I.; Daly, S.; Alcantara, A. R.; Bianchi, D.; Terreni, M.; Ubiali, D. Redesigning the synthesis of vidarabine via a multienzymatic reaction catalyzed by immobilized nucleoside phosphorylases. *RSC Advances* **2015,** *5* (30), 23569-23577, DOI: 10.1039/C4RA15018J.
(38) Huang, X.; Li, M.; Mann, S. Membrane-mediated cascade reactions by enzyme–polymer proteinosomes. *Chemical Communications* **2014,** *50* (47), 6278-6280, DOI: 10.1039/C4CC02256D.
(39) Sutrisna, P. D. C. E. F. o. E. U., Improving the performance of nanocomposite membranes by incorporating inorganic fillers for gas separation. Chen, V. C. E. F. o. E. U., Ed. 2017.
(40) Wong-Ng, W.; Kaduk, J. A.; Espinal, L.; Suchomel, M. R.; Allen, A. J.; Wu, H. High-resolution synchrotron X-ray powder diffraction study of bis(2-methylimidazolyl)-zinc, C8H10N4Zn (ZIF-8). *Powder Diffraction* **2012,** *26* (3), 234-237, DOI: 10.1154/1.3625701.
(41) Shamsaei, E.; Low, Z.-X.; Lin, X.; Mayahi, A.; Liu, H.; Zhang, X.; Zhe Liu, J.; Wang, H. Rapid synthesis of ultrathin, defect-free ZIF-8 membranes via chemical vapour modification of a polymeric support. *Chemical Communications* **2015,** *51* (57), 11474-11477, DOI: 10.1039/C5CC03537F.
(42) Barth, A.; Zscherp, C. What vibrations tell about proteins. *Quarterly Reviews of Biophysics* **2003,** *35* (4), 369-430, DOI: 10.1017/S0033583502003815.
(43) Patra, S.; Hidalgo Crespo, T.; Permyakova, A.; Sicard, C.; Serre, C.; Chausse, A.; Steunou, N.; Legrand, L. Design of metal organic framework-enzyme based bioelectrodes as a novel and highly sensitive biosensing platform. *Journal of Materials Chemistry B* **2015,** *3* (46), 8983-8992, DOI: 10.1039/C5TB01412C.
(44) Ma, F.-f.; Zhang, N.; Wei, X.; Yang, J.-h.; Wang, Y.; Zhou, Z.-w. Blend-electrospun poly(vinylidene fluoride)/polydopamine membranes: self-polymerization of dopamine and the excellent adsorption/separation abilities. *Journal of Materials Chemistry A* **2017,** *5* (27), 14430-14443, DOI: 10.1039/C7TA02845H.

(45) Zhu, M.; Jasinski, J. B.; Carreon, M. A. Growth of zeolitic imidazolate framework-8 crystals from the solid-liquid interface. *Journal of Materials Chemistry* **2012,** *22* (16), 7684-7686, DOI: 10.1039/C2JM30718A.
(46) Pan, Y.; Liu, Y.; Zeng, G.; Zhao, L.; Lai, Z. Rapid synthesis of zeolitic imidazolate framework-8 (ZIF-8) nanocrystals in an aqueous system. *Chemical Communications* **2011,** *47* (7), 2071-2073, DOI: 10.1039/C0CC05002D.
(47) Van Oss, C. J.; Chaudhury, M. K.; Good, R. J. Interfacial Lifshitz-van der Waals and polar interactions in macroscopic systems. *Chemical Reviews* **1988,** *88* (6), 927-941, DOI: 10.1021/cr00088a006.
(48) Moazzam, P.; Tavassoli, H.; Razmjou, A.; Warkiani, M. E.; Asadnia, M. Mist harvesting using bioinspired polydopamine coating and microfabrication technology. *Desalination* **2018,** *429*, 111-118, DOI: 10.1016/j.desal.2017.12.023.
(49) Noorisafa, F.; Razmjou, A.; Emami, N.; Low, Z.-X.; Korayem, A. H.; Kajani, A. A. Surface modification of polyurethane via creating a biocompatible superhydrophilic nanostructured layer: role of surface chemistry and structure. *Journal of Experimental Nanoscience* **2016,** *11* (14), 1087-1109, DOI: 10.1080/17458080.2016.1188223.
(50) Nadar, S. S.; Rathod, V. K. Facile synthesis of glucoamylase embedded metal-organic frameworks (glucoamylase-MOF) with enhanced stability. *International Journal of Biological Macromolecules* **2017,** *95*, 511-519, DOI: 10.1016/j.ijbiomac.2016.11.084.
(51) Zhuang, J.; Kuo, C.-H.; Chou, L.-Y.; Liu, D.-Y.; Weerapana, E.; Tsung, C.-K. Optimized Metal–Organic-Framework Nanospheres for Drug Delivery: Evaluation of Small-Molecule Encapsulation. *ACS Nano* **2014,** *8* (3), 2812-2819, DOI: 10.1021/nn406590q.
(52) Tian, Z.; Yao, X.; Ma, K.; Niu, X.; Grothe, J.; Xu, Q.; Liu, L.; Kaskel, S.; Zhu, Y. Metal-Organic Framework/Graphene Quantum Dot Nanoparticles Used for Synergistic Chemo- and Photothermal Therapy. *ACS omega* **2017,** *2* (3), 1249-1258, DOI: 10.1021/acsomega.6b00385.
(53) Sun, C.-Y.; Qin, C.; Wang, X.-L.; Yang, G.-S.; Shao, K.-Z.; Lan, Y.-Q.; Su, Z.-M.; Huang, P.; Wang, C.-G.; Wang, E.-B. Zeolitic imidazolate framework-8 as efficient pH-sensitive drug delivery vehicle. *Dalton Transactions* **2012,** *41* (23), 6906-6909, DOI: 10.1039/C2DT30357D.
(54) Wang, C.; Wang, L.; Tadepalli, S.; Morrissey, J. J.; Kharasch, E. D.; Naik, R. R.; Singamaneni, S. Ultrarobust Biochips with Metal–Organic Framework Coating for Point-of-Care Diagnosis. *ACS Sensors* **2018,** *3* (2), 342-351, DOI: 10.1021/acssensors.7b00762.
(55) Hedstrom, L.; Szilagyi, L.; J. Rutter, W. *Converting Trypsin to Chymotrypsin: The Role of Surface Loops*, 1992; Vol. 255, p 1249-53.
(56) Nakamura, S.; Ogura, Y. Mode of Inhibition of Glucose Oxidase by Metal Ions. *The Journal of Biochemistry* **1968,** *64* (4), 439-447, DOI: 10.1093/oxfordjournals.jbchem.a128915.
(57) Ghica, M.; Brett, C. *Glucose oxidase inhibition in poly(neutral red) mediated enzyme biosensors for heavy metal determination*, 2008; Vol. 163, p 185-193.
(58) Zhang, Y.; Xie, Z.; Wang, Z.; Feng, X.; Wang, Y.; Wu, A. Unveiling the adsorption mechanism of zeolitic imidazolate framework-8 with high efficiency for removal of copper ions from aqueous solutions. *Dalton Transactions* **2016,** *45* (32), 12653-12660, DOI: 10.1039/C6DT01827K.
(59) Armbruster, D. A.; Pry, T. Limit of Blank, Limit of Detection and Limit of Quantitation. *The Clinical Biochemist Reviews* **2008,** *29* (Suppl 1), S49-S52.
(60) Song, Y.; Qu, K.; Zhao, C.; Ren, J.; Qu, X. Graphene Oxide: Intrinsic Peroxidase Catalytic Activity and Its Application to Glucose Detection. *Advanced Materials* **2010,** *22* (19), 2206-2210, DOI: 10.1002/adma.200903783.

(61) Mu, J.; Wang, Y.; Zhao, M.; Zhang, L. Intrinsic peroxidase-like activity and catalase-like activity of Co3O4 nanoparticles. *Chemical Communications* **2012,** *48* (19), 2540-2542, DOI: 10.1039/C2CC17013B.
(62) Hou, C.; Wang, Y.; Ding, Q.; Jiang, L.; Li, M.; Zhu, W.; Pan, D.; Zhu, H.; Liu, M. Facile synthesis of enzyme-embedded magnetic metal-organic frameworks as a reusable mimic multi-enzyme system: mimetic peroxidase properties and colorimetric sensor. *Nanoscale* **2015,** *7* (44), 18770-18779, DOI: 10.1039/C5NR04994F.
(63) Al-Halhouli, A.; Demming, S.; Alahmad, L.; A, L. I.; Buttgenbach, S. An in-line photonic biosensor for monitoring of glucose concentrations. *Sensors (Basel)* **2014,** *14* (9), 15749-59, DOI: 10.3390/s140915749.
(64) Cocovi-Solberg, D. J.; Miró, M.; Cerdà, V.; Pokrzywnicka, M.; Tymecki, Ł.; Koncki, R. Towards the development of a miniaturized fiberless optofluidic biosensor for glucose. *Talanta* **2012,** *96*, 113-120, DOI: 10.1016/j.talanta.2011.11.021.
(65) Chun, H. J.; Park, Y. M.; Han, Y. D.; Jang, Y. H.; Yoon, H. C. Paper-based glucose biosensing system utilizing a smartphone as a signal reader. *BioChip Journal* **2014,** *8* (3), 218-226, DOI: 10.1007/s13206-014-8308-7.

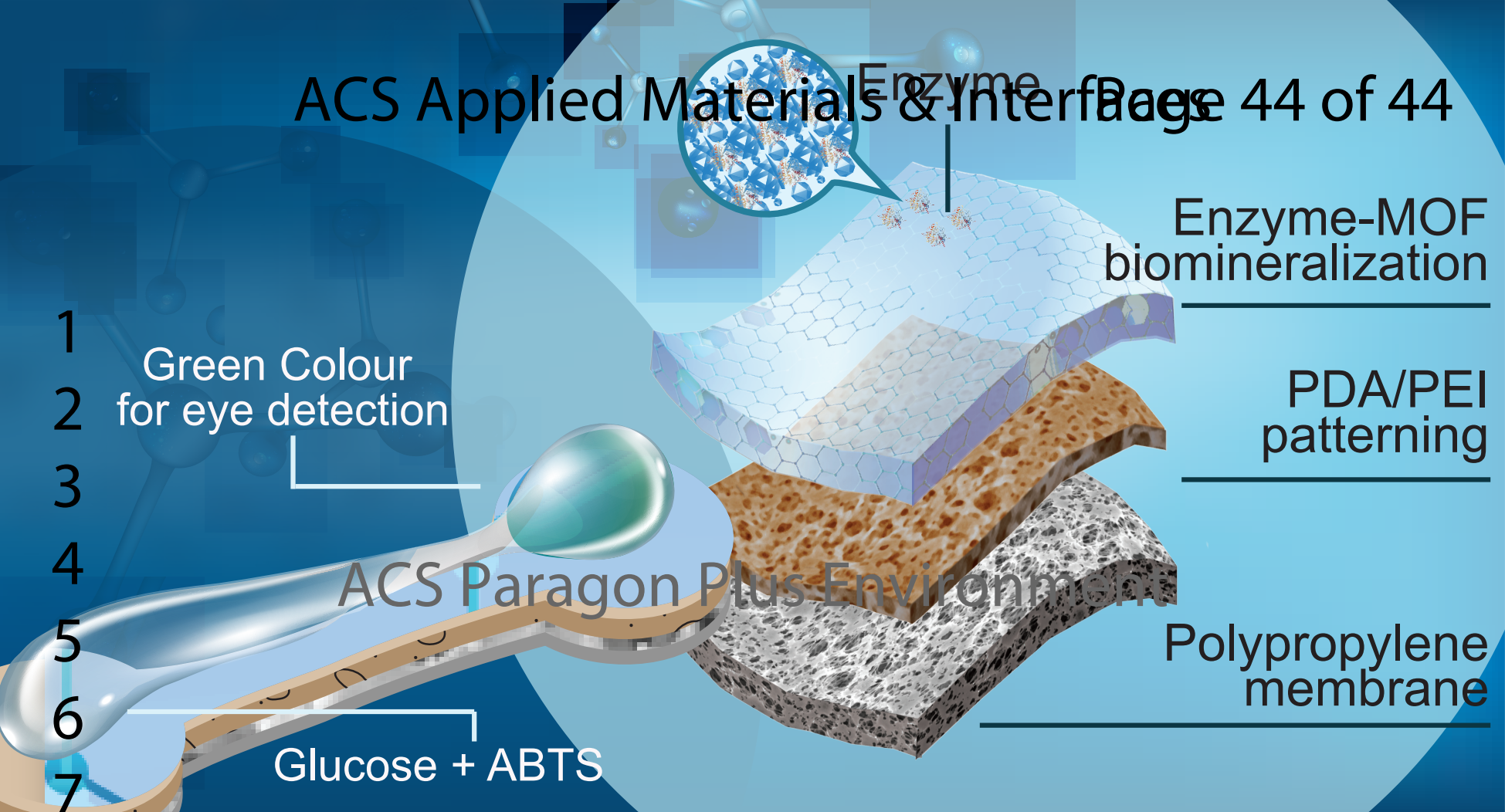
Enzyme
Enzyme-MOF biomineralization
PDA/PEI patterning
Polypropylene membrane
Green Colour for eye detection
Glucose + ABTS
ACS Paragon Plus Environment